Oral transfer of chemical cues, growth proteins and hormones in social insects

LeBoeuf, A.C.[1,2], Waridel, P.[3], Brent, C.S.[4], Gonçalves, A.N. [5,8], Menin, L. [6], Ortiz, D. [6], Riba-Grognuz, O. [2], Koto, A.[7], Soares Z.G. [5,8], Privman, E. [9], Miska, E.A. [8,10,11], Benton, R.*[1] and Keller, L.*[2]

* order decided on a coin-toss as these authors contributed equally.

1. Center for Integrative Genomics, University of Lausanne, CH-1015 Lausanne, Switzerland
2. Department of Ecology and Evolution, University of Lausanne, CH-1005 Lausanne, Switzerland
3. Protein Analysis Facility, University of Lausanne, 1015 Lausanne, Switzerland.
4. Arid Land Agricultural Research Center, USDA-ARS, 21881 N. Cardon Lane, Maricopa, Arizona, 85138, U.S.A.
5. Department of Biochemistry and Immunology, Instituto de Ciências Biológicas, Universidade Federal de Minas Gerais, Minas Gerais, CEP 30270-901, Brasil.
6. Institute of Chemical Sciences and Engineering, Ecole Polytechnique Fédérale de Lausanne, 1015- Lausanne, Switzerland.
7. The Department of Genetics, Graduate School of Pharmaceutical Sciences, The University of Tokyo.
8. Gurdon Institute, University of Cambridge, Tennis Court Road, Cambridge, CB2 1QN, United Kingdom
9. Department of Evolutionary and Environmental Biology, Institute of Evolution, University of Haifa, Haifa 3498838, Israel.Department of Genetics, University of Cambridge, Downing Street, Cambridge, CB2 3EH, United Kingdom
10. Wellcome Trust Sanger Institute, Wellcome Trust Genome Campus, Cambridge, CB10 1SA, United Kingdom

Correspondence to: Adria C. LeBoeuf (Adria.LeBoeuf@gmail.com), Richard Benton (Richard.Benton@unil.ch) or Laurent Keller (Laurent.Keller@unil.ch)

Abstract

Social insects frequently engage in oral fluid exchange – trophallaxis – between adults, and between adults and larvae. Although trophallaxis is widely considered a food-sharing mechanism, we hypothesized that endogenous components of this fluid might underlie a novel means of chemical communication between colony members. Through protein and small-molecule mass spectrometry and RNA sequencing, we found that trophallactic fluid in the ant *Camponotus floridanus* contains a set of specific digestion- and non-digestion related proteins, as well as hydrocarbons, microRNAs, and a key developmental regulator, juvenile hormone. When *C. floridanus* workers' food was supplemented with this hormone, the larvae they reared via trophallaxis were twice as likely to complete metamorphosis and became larger workers. Comparison of trophallactic fluid proteins across social insect species revealed that many are regulators of growth, development and behavioral maturation. These results suggest that trophallaxis plays previously unsuspected roles in communication and enables communal control of colony phenotypes.

Introduction

Many fluids shared between individuals of the same species, such as milk or semen,,can exert significant physiological effects on recipients [1–4]. While the functions of these fluids are well known in some cases [2–5], the role(s) of other socially exchanged fluids (e.g., saliva) are less clear. The context-specific transmission and interindividual confidentiality of socially exchanged fluids raise the possibility that this type of chemical exchange mediates a private means of chemical communication and/or manipulation.

Social insects are an interesting group of animals to investigate the potential role of socially-exchanged fluids. Colonies of ants, bees and termites are self-organized systems that rely on a set of simple signals to coordinate the development and behavior of individual members [6]. While colony-level phenotypes may arise simply from the independent behavior of individuals with similar response thresholds, many group decisions require communication between members of a colony [7]. In ants, three principal means of communication have been described: pheromonal, acoustic, and tactile [8]. Pheromones, produced by a variety of glands, impart diverse information, including nestmate identity and environmental dangers. Acoustic communication, through substrate vibration or the rubbing of specific body parts against one another, often conveys alarm signals. Tactile communication encompasses many behaviors,

from allo-grooming and antennation to the grabbing and pulling of another ant's mandibles for recruitment to a new nest site or resource.

Ants, like many social insects and some vertebrates [9–12], also exhibit an important behavior called trophallaxis, during which liquid is passed mouth-to-mouth between adults or between adults and juveniles. The primary function of trophallaxis is considered to be the exchange of food, as exemplified by the transfer of nutrients from foragers to nurses and from nurses to larvae [13–18]. The eusocial Hymenopteran forgeut has evolved a specialized distensible crop and a restrictive proventriculus (the separation between foregut and midgut) enabling frequent fluid exchange and regulation of resource consumption [19–22]. In addition to simple nourishment, trophallaxis can provide information for outgoing foragers about available food sources [23,24].

Trophallaxis also occurs in a number of non-food related contexts, such as reunion with a nestmate after solitary isolation [25], upon microbial infection [26], and in aggression/appeasement interactions [27]. Furthermore, adult ants have been suggested to use a combination of trophallaxis and allo-grooming to share cuticular hydrocarbons (CHCs) which are important in providing a specific 'colony odor' [9,28], although the presence of CHCs in trophallactic fluid has not been directly demonstrated. Given these food-independent trophallaxis contexts, and the potential of this behavior to permit both 'private' inter-individual chemical exchange as well as rapid distribution of fluids over the social network of a colony, we tested the hypothesis that trophallaxis serves as an additional means of chemical communication and/or manipulation. To identify the endogenous molecules exchanged during this behavior, we used mass-spectrometry and RNA sequencing to characterize the contents of trophallactic fluid, and identified many growth-related proteins, CHCs, small RNAs, and the insect developmental regulator, juvenile hormone. We also obtained evidence that some components of trophallactic fluid can be modulated by social environment, and may influence larval development.

Results

Collection and proteomic analysis of trophallactic fluid

Analysis of the molecules exchanged during trophallaxis necessitated development of a robust method for acquiring trophallactic fluid (TF). We focused on the Florida carpenter ant, *Camponotus floridanus*, which is a large species whose genome has been sequenced [29]. We first attempted to collect fluid from unmanipulated pairs of workers engaged in trophallaxis, but it

was impossible to predict when trophallaxis would occur, and events were usually too brief to collect the fluid being exchanged. We found that after workers were starved and isolated from their colony, then fed a 25% sucrose solution and promptly reunited with a similarly conditioned nestmate, approximately half of such pairs displayed trophallaxis within the first minute of reunion (as observed previously [9,30]), and were more likely to remain engaged in this behavior for many seconds or even minutes. Under these conditions, it was sometimes possible to collect small quantities of fluid from the visible droplet between their mouthparts (referred to as 'voluntary' samples). However, even under these conditions, trophallaxis was easily interrupted, making this mode of collection extremely low-yield.

To obtain larger amounts of TF and avoid the confounding factors of social isolation and feeding status, we developed a non-lethal method to collect the contents of the crop by lightly-squeezing the abdomen of CO_2-anesthetised ants (referred to as 'forced' samples, similar to [26]). This approach yielded a volume of 0.34 ± 0.27 µl (mean ± SD) of fluid per ant. To determine whether the 'forced' fluid collected under anesthesia was similar to the fluid collected from ants voluntarily engaged in trophallaxis, and ensure that it was not contaminated with hemolymph or midgut contents, we also collected samples of these four fluid sources. To compare the identities and quantities of the different proteins found in each fluid, all samples were analyzed by nanoscale liquid chromatography coupled to tandem mass spectrometry (nano-LC-MS/MS) (Fig. 1A).

Hierarchical clustering of normalized spectral counts of the proteins identified across our samples revealed high similarity between voluntary and forced TF, but a clear distinction of these fluids from midgut contents or hemolymph (Fig. 1A, for protein names and IDs see Figure 1-figure supplement 1). While the voluntary TF samples contained fewer identified proteins than the forced TF samples – likely due to lower total collected TF volume per analyzed sample (<1 µl vs. >10 µl) – the most abundant proteins were present across all samples in both methods of collection (Fig. 1A). To investigate whether the few differences observed between the voluntary and forced TF in the less abundant proteins might be due to the starvation and/or social isolation conditions used to collect voluntary TF, we isolated groups of 25-30 ants from their respective queens and home colonies for 14 days, with constant access to food and water, and collected TF both directly before and after the period of isolation. Social isolation affected the ratios of proteins in TF, with 5 of the top 40 proteins in TF becoming significantly less abundant and one more abundant when ants were socially isolated (Fig. 1B; see Figure 1-figure supplement 2 for names and IDs). Three of the proteins down-regulated in social isolation were also significantly less abundant in voluntary TF samples (from socially isolated ants) relative to

forced TF samples (from within-colony ants, Figure 1-figure supplement 2). Together these results provide initial evidence that the composition of this fluid is influenced by social and/or environmental experience of an ant, and support the validity of our methodology to force collect TF.

Of the 50 most abundant proteins found in TF (Fig. 1C), many are likely to be digestion-related (*e.g.,* three maltases, one amylase, various proteases, two glucose dehydrogenases, one DNase) and three Cathepsin D homologs might have immune functions [26]. However, at least ten of the other proteins have putative roles in the regulation of growth and development, including two hexamerins (nutrient storage proteins [31]), a yellow/major royal jelly protein (MRJP) homolog (likely nutrient storage [32]) and an apolipophorin (vitellogenin-domain containing lipid-transport protein [33]). Most notably, TF contained several proteins that are homologous to insect juvenile hormone esterases (JHEs) and Est-6 in *Drosophila melanogaster* (Fig. 1D). JHEs are a class of carboxylesterases that degrade the developmental regulator, juvenile hormone (JH) [34,35], and Est-6 is an abundant esterase in *D. melanogaster* seminal fluid [36–38]. While most insects have only one or two JHE-like proteins [35,39], *C. floridanus* has an expansion of more than ten related proteins, eight of which were detected in TF (Fig. 1D, Figure 1-figure supplement 1, 2) and two in hemolymph (Figure 1-figure supplement 1). Three of the abundant JHE-like proteins are significantly down-regulated in the TF of ants that have undergone social isolation (Figure 1-figure supplement 2).

Thirty-three of the 50 most abundant TF proteins had predicted N-terminal signal peptides, suggesting they can be secreted directly into this fluid by cells lining the lumen or glands connected to the alimentary canal (Figure 5-supplement 2). Moreover, half of the proteins without such a secretion signal had gene ontology terms indicating extracellular or lipid-particle localization, which suggests that they may gain access to the lumen of the foregut through other transport pathways.

Trophallaxis microRNAs

Many small RNAs have been found in externally-secreted fluids across taxa, such as seminal fluid, saliva, milk and royal jelly [40–42]. Although the functions of extracellular RNAs remain unclear [43], we investigated if TF also contains such molecules by isolating and sequencing small RNAs from *C. floridanus* TF. After filtering out RNA corresponding to potential commensal microorganisms (including the known symbiont, *Blochmannia floridanus*; Supplementary File 1) and other organic food components, we detected 64 miRNAs. Forty-six of these were identified based upon their homology to miRNAs of the honey bee *Apis mellifera* [42,44,45], while 18

sequences (bearing the structural stem-loop hallmarks of miRNA transcripts) were specific to *C. floridanus* (Fig. 2, Figure 2-source data 1). The most abundant of the 64 miRNAs was miR-750, followed by three *C. floridanus*-specific microRNAs. The role of miR-750 is unknown, but the expression of an orthologous miRNA in the Asian tiger shrimp, *Penaeus monodon*, is regulated by immune stress [46]. Notably, sixteen of the miRNAs detected in the *C. floridanus* TF are also present in *A. mellifera* worker jelly and/or royal jelly [42], which are oral secretion fed to larvae to bias them toward a worker or queen fate.

Trophallactic fluid contains long-chain hydrocarbons

Trophallaxis has long been suggested to contribute to the exchange and homogenization of colony odor [47]. The observation that different ant species have distinct blends of non-volatile, cuticular hydrocarbons (CHCs) – which also display quantitative variation within species – have made these chemicals prime candidates for conveying nestmate recognition cues [48–53]. CHC profiles of ants within a colony are similar, while individuals isolated from their home colony often vary in their CHC make-up [54], suggesting that the profiles are constantly unified between nestmates [9]. However, it remains unclear if CHCs are exchanged principally by trophallaxis, or through other mechanisms such as allo-grooming and contact with the nest substrate [9,28,49]. We therefore investigated whether CHCs are present in TF, and how they relate to those present on the cuticle. To do this, we analyzed by gas chromatography mass spectrometry (GC-MS) the TF and cuticular extracts collected from the same five groups of 20-38 workers.

We identified 63 molecules in TF (Table 1), including eight fatty acids and fatty acid esters, 13 unbranched and 36 branched hydrocarbons with one to five methyl branches. The majority (40/63) of the TF compounds comprised 27 or more carbons. Cuticular extracts also contained predominantly multiply branched alkanes with 27 or more carbons, corresponding to previous observations of CHCs in this species [48,55] (Fig. 3). All of the highly abundant hydrocarbons in TF (marked in Fig. 3) were also present on the cuticle of the workers analyzed, supporting the potential for trophallaxis to mediate inter-individual CHC exchange. Moreover, there was a significantly greater (t-test, $p < 0.0003$) similarity across colonies in the hydrocarbon profiles of TF than hydrocarbon profiles of the cuticle (similarity was measured by cross-correlation between GC-MS profiles, Fig 3D-E). Altogether, these observations indicate that while CHCs are likely to be exchanged by trophallaxis, additional mechanisms are probably involved in generating the colony-specific bouquet of these compounds.

Juvenile Hormone is exchanged through trophallaxis and can influence larval development

Given the abundance of the expanded family of JHE-like proteins in TF, we determined whether JH itself is also present in this fluid. The primary JH found in Hymenoptera, JH III, is thought to circulate in the hemolymph after being produced by the corpora allata [56]. To detect and quantify JH in both TF and hemolymph, we employed a derivatization and purification process prior to GC-MS analysis [57–59]. While both sets of measurements were highly variable across samples, we found high levels of JH in TF with concentrations of the same order of magnitude as those found in hemolymph (Fig. 4A).

Because JH is an important regulator of development, reproduction, and behavior [60], we investigated whether the dose of JH that a larva receives by trophallaxis with a nursing worker might be physiologically relevant. If an average worker has approximately 0.34 µL of TF in her crop at a given time (as measured in our initial experiments; see above), this corresponds to a dose of approximately 31 pg of JH. The analysis of 35 larvae collected midway through development (i.e., third instar out of four worker instars, mean ± SD: 4.0 ± 0.19 mm long and 1.4 ± 0.12 mm wide) revealed that they contained 100-700 pg of JH (Fig. 4B). Thus, the amount of JH received during an average trophallaxis event amounts to ~5-31% of the JH content of a third instar larva. While it is difficult to determine how much of the JH fed to larvae remains in the larval digestive tract, these results indicate that there is potentially sufficient JH in a single trophallaxis-mediated feeding to shift the titer of a recipient larva.

We next determined whether adding exogenous JH to the food of nursing workers could change the growth of the reared larvae. We created groups of 25-30 workers and allowed them to each rear 5-10 larvae to pupation, in the presence of food and sucrose solution that was supplemented with either JH or only a solvent. Larvae reared by JH-supplemented workers grew into larger adults than those reared by solvent-supplemented controls (Fig. 4C, GLMM, $p < 9.01e^{-06}$). Moreover, larvae reared by JH-supplemented caretakers were twice as likely to successfully undergo metamorphosis relative to controls (Fig. 4D, binomial GLMM, $p < 7.39e^{-06}$). These results are consistent with previous studies in other species of ants and bees using methoprene (a non-hydrolyzable JH analog), whose external provision to the colony can lead to larvae developing into larger workers and even queens [60–62].

Comparative proteomics reveals species-specific growth-regulatory proteins in trophallactic fluid

To expand our survey of TF, we collected this fluid from other species of social insects: a closely related ant (*C. fellah),* an ant from another sub-family (the fire ant *Solenopsis invicta),* and the bee *A. mellifera*. Nano-LC-MS/MS analyses identified 79, 350, and 136 proteins in these three species respectively (84 were identified in *C. floridanus*). We assigned TF proteins from all four analyzed species to 138 distinct groups of predicted orthologous proteins (see Methods); of these, 72 proteins were found in the TF of only one species (Fig. 5, Figure 5-source data 1).

Only eight ortholog groups contained representatives present in the TF of all four species (Fig. 5B). Most of these appear to have functions related to digestion, except for apolipophorin, which is involved in lipid/nutrient transport [33]. For ortholog groups found in the TF of the three ant species, most were also digestion-related with the notable exception of CREG1, a secreted glycoprotein that has been implicated in cell growth control [63] and insect JH response [64–66]. Genus- and species-specific proteins were frequently associated with growth or developmental roles. For example, *A. mellifera* TF contained 12 distinct major royal jelly proteins (MRJP) thought to be involved in nutrient storage and developmental fate determination [32,67], while *S. invicta* TF contained a highly abundant JH-binding protein and a vitellogenin. The two *Camponotus* species shared many orthologous groups, consistent with their close phylogenetic relationship. Five of the seven JHE/Est-6 proteins found in *C. floridanus* TF also had orthologs present in *C. fellah* TF. Additionally, these two species shared a MRJP/Yellow homolog, and an NPC2-related protein, which, in *D. melanogaster*, is involved in sterol binding and ecdysteroid biosynthesis [68]. Finally, 26 ortholog groups were found in multiple species, but not the most closely related ones (*e.g., A. mellifera* and *S. invicta,* or *S. invicta* and only one of the two *Camponotus* species). One-third of these were associated with growth and developmental processes (e.g., three hexamerins, two MRJP/yellow proteins, imaginal disc growth factor 4, vitellogenin-like Vhdl and an additional NPC2). Together these analyses indicate that approximately half of all TF protein ortholog groups appear to be digestion-related, consistent with TF being composed of the contents of the foregut. However, many TF proteins have putative roles in growth, nutrient storage, or the metabolism and transport of JH, vitellogenin or ecdysone.

Discussion

We have characterized the fluid that is orally exchanged during trophallaxis, a distinctive behavior of eusocial insects generally considered as a means of food sharing. Our results reveal that the transmitted liquid contains much more than food and digestive enzymes, and

236 includes non-proteinaceous and proteinaceous molecules implicated in chemical discrimination
237 of nestmates, growth and development, and behavioral maturation. These findings suggest that
238 trophallaxis underlies a private communication mechanism that can have multiple phenotypic
239 consequences. More generally, our observations open the possibility that exchange of oral
240 fluids (e.g., saliva) in other animals might also serve functions not previously suspected [69,70].
241 In ants, trophallaxis has long been thought to be a mode of transfer for the long-chain
242 hydrocarbons that underlie nestmate recognition [9,30,51,53,71,72]. However, previous work
243 has analyzed only the passage of radio-labeled hydrocarbons between individuals [9,30,71] and
244 between individuals and substrates [49]. Without explicitly sampling the contents of the crop, it
245 is not possible to differentiate between components passed by trophallaxis or by physical
246 contact. Our study is, to our knowledge, the first to demonstrate that TF contains endogenous
247 long-chain hydrocarbons. Interestingly, we found differences in the hydrocarbon profiles of the
248 TF and the cuticle of the same ants, suggesting the existence of other processes regulating the
249 relative proportion of CHCs and/or additional sources of these compounds. Further work
250 manipulating and comparing hydrocarbon profiles of TF and cuticle of multiple individual ants
251 within the same colony is necessary to understand the impact of the observed variation in TF
252 and cuticular hydrocarbons.
253 Consistent with the view that the gut is one of the first lines of defense in the body's
254 interface with the outside world [73,74], the four TF proteomes analyzed in this study include
255 many potential defense-related proteins. Homologs of the Cathepsin D family of proteins, which
256 have been implicated in growth, defense and digestion [75,76], were present in the TF of both
257 *Camponotus* species. Prophenoloxidase 2, an enzyme responsible for the melanization involved
258 in the insect immune response [74], was found in the TF of *A. mellifera and S. invicta.* All four
259 species contained several members of the serine protease and serpin families, which have well-
260 documented roles in the prophenoloxidase cascade and more general immune responses in *D.*
261 *melanogaster* and other animals [73,77]. The TF of two species had orthologs of the recognition
262 lectin GNBP3 which is also involved in the prophenoloxidase cascade. Finally, a handful
263 chromatin-related proteins (e.g., histones, CAF1) were found in *S. invicta*, and to a lesser extent
264 in the other two ants. Their presence may simply reflect a few cells being sloughed from the
265 lumen of the foregut, or could be indicative of a defense process termed ETosis, whereby
266 chromatin is released from the nuclei of inflammatory cells to form extracellular traps that kill
267 pathogenic microbes [78,79].
268 The presence of development- and growth-related components in the TF of diverse
269 social insects suggests that this fluid may play a role in directing larval development. Previous

work has shown that the developmental fate of larvae and the process of caste determination in various ant and bee species can be influenced by treating colony members with JH or JH analogs [18,62,80–82]. Moreover, in some species, workers play an important role in regulating caste determination [67,83–85] but it is unknown how workers might influence the JH titers of larvae. Our finding that TF contains JH raises the possibility of trophallaxis as a direct means by which larval hormone levels and developmental trajectories can be manipulated. This type of mechanism has some precedent: honey bee workers bias larval development toward queens by feeding royal jelly to larvae, an effect that might be mediated by MRJPs [67,86–88]. Across the TF of four species of social insect, we have found diverse molecules intimately involved in insect growth regulation: JH, JHE, JH-binding protein, vitellogenin, hexamerin, apolipophorin, and MRJPs. Several of the proteins and microRNAs identified in ant and bee TF are also found in royal and worker jelly [42,66]. Notably, there are also some similarities between proteins in social insect TF and mammalian milk [89], such as the cell growth regulator CREG1. The between-genera variation in the most abundant growth-related proteins (e.g., MRJPs in honey bee, JH-binding protein and hexamerins in fire ant, and JHEs in *Camponotus*) indicates that there might be multiple evolutionary origins and/or rapid divergence in trophallaxis-based signals potentially influencing larval growth.

The finding that TF contains many proteins, miRNAs, CHCs and JH raises the question of how they come to be present in this fluid. Many non-food-derived components in TF are likely to be either directly deposited into the alimentary canal: over two-thirds of the proteins present in TF had a predicted signal peptide suggesting that they are probably secreted by the cells lining the foregut or glands connected to the alimentary canal (e.g., postpharyngeal, labial, mandibular, salivary glands). Additionally, TF molecules are likely to be acquired by transfer among nestmates through licking, grooming, and trophallaxis. For example, CHCs are produced by oenocytes, transmitted to the cuticle, ingested, and sequestered in the postpharyngeal gland [49,53,90]. Interestingly, JH is synthesized in the corpora allata, just caudal to the brain [91]. Although the mechanisms of JH uptake by tissues are still incompletely understood [92–95], the TF proteins apolipophorin, hexamerin, JH-binding protein and vitellogenin have all been implicated in JH binding and transport between hemolymph and tissues [91,93–96], and these factors may be responsible for transporting JH into the foregut. Unfortunately, even in *Drosophila* mechanisms of JH uptake by tissues are still unclear [93–95,92]. Extracellular miRNAs are secreted and transported through a variety of pathways, but the functional relevance of such molecules is still controversial [40,97,98,44,99].

While the simultaneous presence of JH and a set of putative JH degrading enzymes (the JHE/Est-6 family) in *C. floridanus* TF may appear surprising, there are at least two possible explanations. First, this might reflect a regulatory mechanism of JH level at the individual and colony levels. Many biological systems use such negative feedback mechanisms to buffer signals and enable rapid responses to environmental change [100]. Alternatively, these enzymes may have evolved a different function along with their novel localization in TF. In other insects JHE-related enzymes are typically expressed in the fat body and circulate in the hemolymph [101–103]. ,The expansion of JHE-like proteins in *C. floridanus* was accompanied by a high specificity in their localization, with two (E2AM67, E2AM68) being present exclusively in the hemolymph, and four (E2ANU0, E2AI90, E2AJM0, E2AJL9) exclusively in TF. This coexistence of JH and JHEs reveals a striking parallel with the constituents of a different socially-exchanged fluid in *D. melanogaster*. *Drosophila* Est-6 is highly abundant in seminal fluid, together with its presumed substrate, the male-specific pheromone 11-*cis*-vaccenyl acetate (cVA). cVA has multiple roles in influencing sexual and aggressive interactions and its transfer to females during copulation potently diminishes her attractiveness to future potential mates [1,104,105].

Given that larvae are fed JH and food, and both are necessary for development, a future goal will be to dissect the relative contribution and potential synergy of these components. Furthermore, JH has many other functions in social insects, including behavioral modulation, longevity, fecundity and immunity [106–109]; the relevance of trophallaxis-mediated JH exchange between adults remains to be explored. Considering that most, if not all, individuals in a colony must share food through trophallaxis, it will also be of interest to understand if and how individual-, or caste-specific TF-based information signals emerge. Recent work on trophallaxis networks [10] and interaction networks [110], indicate that ants preferentially interact with others of similar behavioral type (e.g., nurses with nurses, and foragers with foragers). This raises the possibility that different pools of TF with different qualities exist. A key challenge will be to develop specific genetic and/or pharmacological tools to test the biological relevance of molecules transmitted by trophallaxis.

Fig 1 Proteomic characterization of *Camponotus floridanus* trophallactic fluid.
(A) Heat map showing the percentage of total molecular weight-normalized spectra assigned to proteins from hemolymph, voluntary TF, forced TF or midgut fluids (normalized spectral abundance factor, NSAF [111]). C1-C10 indicate colony of origin. Forced trophallaxis samples are pooled from 10-20 ants, hemolymph from 30 ants, and the contents of dissected midguts from 5 ants each. Voluntary and midgut samples were collected from ants of multiple colonies; multiple samples are differentiated by letters. Approximately unbiased (AU) bootstrap probabilities for 10,000 repetitions are indicated by black circles where greater or equal to 95%.
(B) Trophallaxis samples from the same ants, in-colony and group-isolated. Trophallactic fluids were sampled first upon removal from the colony, then after 14 days of group isolation (20-30 individuals per group). Values were compared by spectral counting, and the dendrogram shows approximately unbiased probabilities for 10,000 repetitions. Along the right side, asterisks indicate Bonferroni-corrected t-test significance to $p < 0.05$ between in-colony and isolated TF. Approximately unbiased (AU) bootstrap probabilities for 10,000 repetitions are indicated by black circles where greater or equal to 95%.
(C) The most abundant proteins present in TF sorted by natural-log-scaled NSAF value. The UniProt ID or NCBI ID is listed to the right.
(D) A dendrogram of proteins including all proteomically observed juvenile hormone esterases (JHE)/Est-6 proteins in *C. floridanus*, the orthologs in *D. melanogaster* and *A. mellifera*, and biochemically characterized JHEs. Each protein name is followed by the UniProt ID. *C. floridanus* JHE/Est-6 proteins are listed with the fluid source where they have been found. Names are color-coded by species. Bootstrap values >95% are indicated with a black circle. JHE/Est-6 6 (E2AJL7) is identified by PEAKS software but not by Scaffold, and consequently is not shown in the proteomic quantifications in panels (A-C).

Figure 1–figure supplement 1
Proteomic characterization of *C. floridanus* fluid compartments with UniProt IDs listed to the left and protein names to the right.

Figure 1–figure supplement 2
Trophallaxis samples from the same ants, in-colony and group-isolated. Trophallactic fluid of groups of ant workers sampled first upon removal from the colony, then after 14 days of group isolation (20-30 individuals per group). Values were normalized using spectral counting, and the dendrogram shows approximately unbiased probabilities for 10,000 repetitions. Along the right side, UniProt IDs are shown. Proteins that significantly decrease in abundance in isolation are shown in orange, and proteins that increase in abundance are shown in green (t-test $p < 0.05$).

Asterisks indicate Bonferroni-corrected t-test significance. Names in bold italics indicate proteins that significantly decreased in abundance in voluntary samples (socially isolated, starved then fed) relative to forced TF samples (in-colony) from data shown in Fig. 1A and figure supplement 1. Approximately unbiased (AU) bootstrap probabilities for 10,000 repetitions are indicated by black circles where greater or equal to 95% and grey circles where greater or equal to 75%.

Fig 2 Trophallactic fluid of *C. floridanus* contains microRNAs. Left: heatmap showing the length of reads assigned to each *C. floridanus* microRNA (miRNA) found in TF. MiRNAs should exhibit a consistent read size typically between 18 and 22 base pairs. Right: histogram indicating read abundance. miRNA names were assigned through homology to *A. mellifera* where possible. Letters were assigned for novel miRNA. Bold miRNA names indicate miRNAs whose homologs were also observed in royal and/or worker jelly in *A. mellifera* [42]. Source data in Figure 2-source data 1.

Table 1.

Table of all components identified by GC-MS in TF of *C. floridanus*. Table of all components identified by GC-MS in TF. Molecules marked with black dots (•) were found only in TF and not on the cuticle.

Retention Time	Proposed MF	Proposed structure	RI	Peak ID
13.35	$C_{15}H_{32}$	Pentadecane	1500	
14.05	$C_{16}H_{34}$	4-Methyltetradecane	1600	
14.34	$C_{10}H_{10}O_3$	Mellein	1674	
15.05	$C_{16}H_{34}$	Hexadecane	1600	
16.47	$C_{17}H_{36}$	Heptadecane	1700	
17.06	$C_{20}H_{42}$	7,9-Dimethylheptadecane	1710	
17.83	$C_{18}H_{38}$	Octadecane	1800	
19.15	$C_{19}H_{40}$	Nonadecane	1900	
19.89	$C_{21}H_{44}$	7,10,11-Trimethyloctadecane	1920	
19.97	$C_{16}H_{32}O_2$	n-Hexadecanoic acid	1962	
20.5	$C_{18}H_{36}O_2$	Ethyl palmitate	1968	
20.62	$C_{20}H_{42}$	Eicosane	2000	
20.98	$C_{18}H_{36}O$	Octadecanal	1999	
22.89	$C_{18}H_{32}O_2$	Linoleic acid	2133	
23.03	$C_{18}H_{34}O_2$	Oleic acid	2179	•
23.46	$C_{20}H_{36}O_2$	Ethyl-9-Cis-11-Trans-octadecadienoate	2193	
23.59	$C_{20}H_{38}O_2$	Ethyl oleate	2173	•
24.3	$C_{22}H_{46}$	Docosane	2200	

26.27	$C_{23}H_{46}$	7Z-Tricosene	2296	•
26.45	$C_{20}H_{38}O_2$	Cis-13-Eicosenoic acid	2368	
29.08	$C_{24}H_{50}$	Tetracosane	2400	
32.51	$C_{25}H_{52}$	Pentacosane	2500	
34.69	$C_{26}H_{54}$	Hexacosane	2600	
36.37	$C_{27}H_{56}$	4-Methylhexacosane	2640	
36.91	$C_{27}H_{54}$	Heptacosene	2672	
38.76	$C_{28}H_{58}$	9-Methylheptacosane	2740	
39.19	$C_{28}H_{58}$	5-Methylheptacosane	2740	
40.05	$C_{28}H_{58}$	*-Trimethylpentacosane	2610	
40.63	$C_{28}H_{58}$	Octacosane	2800	
40.76	$C_{28}H_{58}$	7-Methylheptacosane	2753	
41.36	$C_{29}H_{60}$	5,7,11-Trimethylhexacosane	2783	
41.88	$C_{29}H_{60}$	4-Methylnonacosane	2810	
42.23	$C_{29}H_{58}$	Nonacosene	2875	
42.47	$C_{30}H_{62}$	2,10-Dimethyloctacosane	2874	G
42.7	$C_{29}H_{60}$	Nonacosane	2900	H
42.9	$C_{31}H_{64}$	9,16-Dimethylnonacosane	2974	
43.29	$C_{31}H_{64}$	9,20-Dimethylnonacosane	2974	
43.36	$C_{30}H_{62}$	7-Methylnonacosane	2940	
43.51	$C_{31}H_{64}$	4-Methyltriacontane	3045	
43.79	$C_{31}H_{64}$	7,16-Dimethylnonacosane	2974	
43.9	$C_{31}H_{64}$	2-Methyltriacontane	3045	E
43.96	$C_{31}H_{64}$	10-Methyltriacontane	3045	K
44.12	$C_{32}H_{66}$	10,11,15-Trimethylnonacosane	3023	
44.42	$C_{32}H_{66}$	*-Dimethyltriacontane	3083	B
44.74	$C_{32}H_{66}$	8,12-Dimethyltriacontane	3083	Q
45.02	$C_{33}H_{68}$	*-Trimethyltriacontane	3119	R
45.3	$C_{31}H_{62}$	Hentriacontene	3100	
45.45	$C_{33}H_{68}$	5,10,19-Trimethyltriacontane	3119	S
45.54	$C_{27}H_{46}O$	Cholest-5-en-3-ol / Cholesterol	3100	A
45.7	$C_{31}H_{64}$	Hentriacontane	3100	M
46	$C_{34}H_{70}$	9,13-Dimethyldotriacontane	3185	C
46.56	$C_{33}H_{68}$	5,9-Dimethyldotriacontane	3185	D
46.69	$C_{34}H_{70}$	*-Tetramethylnonacosane	3160	J
46.93	$C_{34}H_{70}$	*-Multiramified tetratriacontane	3220-3100	O
47.15	$C_{34}H_{70}$	5,9,13,17,21-Pentamethylnonacosane	3100	N
47.28	$C_{33}H_{68}$	*-Dimethylhentriacontane	3185	T
47.58	$C_{34}H_{70}$	10,14,18,22-Tetramethyldotriacontane	3160	P

48.01	$C_{34}H_{70}$	*-Tetramethyldotriacontane	3160	
48.12	$C_{35}H_{72}$	11,15-Dimethyltritiacontane	3380	F
48.77	$C_{35}H_{72}$	*-Methyltetratriacontane	3440	L
49.54	$C_{36}H_{74}$	14-Methylpentatriacontane	3540	
49.67	$C_{36}H_{74}$	*-Multiramifiedhexatriacontane	3420-3300	
50.28	$C_{37}H_{76}$	*-Tetramethyltetratriacontane	3480	

Fig 3 Trophallactic fluid of *C. floridanus* contains cuticular hydrocarbons.

(A-B) Gas chromatography-mass spectrometry profiles in the retention time window for cuticular hydrocarbons (C28-C37), from hexane extracts of whole body (A) and from trophallactic fluid (B). Samples were extracts from whole body and trophallactic fluid for five groups of 20-38 ants. Each group of ants is from a different colony, C11-C15. Different colonies are shown in distinct colors. Source data in Figure 3-source data 1. The abundant component (peak A) found in TF samples but not on the cuticle was cholesterol, a molecule that insects cannot synthesize but must receive from their diet. Three molecules outside this window were found only in TF and not on the cuticle: 7Z-tricosene, oleic acid, ethyl oleate (Table 1). All have been reported to be pheromones in other insect species [112–115].

(C) A hierarchically clustered heatmap of the dominant peaks in the range of retention times for long-chain cuticular hydrocarbons. The dendrogram shows approximately unbiased probabilities for 10,000 repetitions, and approximately unbiased bootstrap values are color-coded where >95% are indicated with black circles. Letters along the right correspond to individual peaks in (A) and (B).

(D) Normalized pair-wise cross-correlation values for each TF and body hydrocarbon profile for each of the five colonies. Source data in Figure 3-source data 2.

(E) Normalized pair-wise cross-correlation values between TF hydrocarbon profiles and between body hydrocarbon profiles indicate that the TF hydrocarbon profiles are significantly more similar than are body hydrocarbon profiles. Median values and interquartile ranges are shown. t-test, $p < 0.0003$.

Figure 3-figure supplement 1

(A) Typical GC-MS chromatogram of a TF sample, showing the main hydrocarbons C28-C37 eluting after 40 min. The insert shows the region with minor hydrocarbons C15-C28.

(B-D) GC-MS Mass spectra of linear alkane (n-hexacosane at Rt 34.69 min, panel B) and a dimethylated alkane at Rt 43.29 min (C). Extracted MS profiles were fitted with an exponential

412 decay equation (B, D). The proposed structure for the branched alkane based on fragments
413 ions (141 and 309) is 9,20-dimethyl nonacosane (D).
414 (E) Retention index (RI) values vs. number of carbons extracted from the NIST Chemistry
415 WebBook library, depending on the number of ramifications: linear (black), monomethyl (red),
416 dimethyl (blue), trimethyl (pink), tetramethyl (green) and pentamethyl (dark blue).
417 (F) The black dots represent experimental retention times with the calculated RI index for all
418 identified hydrocarbons of the TF sample. The red dots represent the experimental retention
419 times and with their RI index for the linear C8-C40 alkane standard.
420
421 **Fig 4. Juvenile Hormone passed in trophallactic fluid increases larval growth and rate of**
422 **pupation in *C. floridanus*.**
423 (A) JH titer in trophallactic fluid and hemolymph (n=20; each replicate is a group of 30 workers).
424 Source data in Figure 4-source data 1.
425 (B) JH content of third instar larvae. Source data in Figure 4-source data 2.
426 (C) Head width of pupae raised by workers who were fed food supplemented with JH III or
427 solvent. General linear mixed model (GLMM) testing effect of JH on head width with colony,
428 replicate and experiment as random factors, *** $p < 9.01e^{-06}$. Source data in Figure 4-source
429 data 3.
430 (D) Proportion of larva that have undergone metamorphosis when workers were fed food
431 supplemented with JH III or solvent only. Binomial GLMM testing effect of JH on survival past
432 metamorphosis with colony and experiment as random factors, *** $p < 7.39e^{-06}$.
433 Median values and interquartile ranges are shown in panels (A-C). Panels (C) and (D) are data
434 from three separate experiments where effects in each were individually significant to $p < 0.05$.
435 Source data in Figure 4-source data 4.
436
437 **Fig 5. Proteins in trophallactic fluid across social insect species.**
438 (A) Venn diagram indicating the number of species-specific and orthologous proteins detected
439 in TF from the indicated species, whose phylogenetic relationships are shown with black lines.
440 (B) Heat maps showing the percentage of total molecular-weight normalized spectra in TF
441 samples assigned to the proteins in each given species, averaged over all in-colony samples for
442 that species. Samples sizes: *C. floridanus* (n=15), *C. fellah* (n=6), *S. invicta* (n=3), *A. mellifera*
443 (n=6).

(C) Species-specific TF proteins. The 26 TF ortholog groups found in two or three species, but not the most closely related ones (e.g., *A. mellifera* and *S. invicta,* or *S. invicta* and only one of the two *Camponotus* species) are indicated in Figure 5–figure supplement 1.

Figure 5–figure supplement 1

Heat maps showing the percentage of total molecular-weight normalized spectra in trophallactic fluid samples assigned to each protein in three ant species and the European honey bee, averaged over all in-colony samples for that species. Sample sizes: *C. floridanus* (n=15), *C. fellah* (n=6), *S. invicta* (n=3), *A. mellifera* (n=6). The 26 TF ortholog groups found in two or three species, but not the most closely related ones (e.g., *A. mellifera* and *S. invicta,* or *S. invicta* and only one of the two *Camponotus* species) are shown in orange. Protein names are shown on the left. Identifiers can be found in the table in Figure 5–source data 1.

Figure 5-source data 1. A table of all orthologous proteins and, where known, their putative functions, identifiers, *D. melanogaster* orthologs, presence of annotated secretion signals and average NSAF values when present in TF. A complete orthology across the four species can be found in Supplementary File 3.

Materials and methods

Insect source and rearing

Camponotus floridanus workers came from 16 colonies established in the laboratory from approximately one-year old founding queens and associated workers collected from the Florida Keys in 2006, 2011 and 2012. Ants were provided with sugar water, an artificial diet of honey or maple syrup, eggs, agar, canned tuna and a few *D. melanogaster* once a week. Maple syrup was substituted for honey and no *Drosophila* were provided in development and proteomic experiments to avoid contamination with other insect proteins. Colonies were maintained at 25°C with 60% relative humidity and a 12 h light:12 h dark cycle. *Camponotus fellah* colonies were established from queens collected after a mating flight in March 2007 in Tel Aviv, Israel (Colonies #5, 28, 33). The ant colonies were maintained at 32°C with 60% relative humidity and a 12 h light:12 h dark cycle. Fire ant workers (*Solenopsis invicta*) were collected from three different colonies, two polygyne, one monogyne, maintained at 32°C with 60% relative humidity and a 12 h light:12 h dark cycle. Honeybee workers (*Apis mellifera*, Carnica and Buckfast) were collected from six different hives maintained with standard beekeeping practices.

Fluid Collection

'Voluntary' TF was collected from individuals who had been starved and socially isolated for 1-3 weeks, then fed 25% sucrose solution, and promptly re-introduced to other separately isolated nestmates. Ants were monitored closely for trophallaxis events; when one had begun, a pulled glass pipette was brought between the mouthparts of the 2-4 individuals and fluid was intercepted. Typically this stopped the trophallaxis event, but on rare occasions it was possible to acquire up to sub-microliter volumes of TF.

For 'forced' collection, ants were anesthetized by CO_2 (on a CO_2 pad; Flypad, FlyStuff) and promptly flipped ventral-side up. The abdomen of each ant was lightly squeezed with wide insect forceps to prompt the regurgitation of fluids from the social stomach. Ants that underwent anesthesia and light squeezing yielded on average 0.25 µl of fluid and recovered in approximately 5 min. TF was collected with graduated borosilicate glass pipettes, and transferred immediately to either buffer (100 mM NaH_2PO_4, 1 mM EDTA, 1 mM DTT, pH 7.4) for proteomic experiments, to RNase-free water for RNA analyses, or to pure EtOH for GC-MS measurements. TF was collected from *C. fellah* and *S. invicta* in the same manner as from *C. floridanus*; for *S. invicta* 100-300 ants were used due to their smaller body size and crop volume.

493 Honey bee TF was collected from bees that were first cold-anesthetized and then
494 transferred to a CO_2 pad to ensure continual anesthesia during collection of TF as described
495 above. Honey bees yielded higher volumes of TF than did ants (0.94 µl TF per honey bee,
496 SD=0.54 relative to 0.34 µl TF per *C. floridanus* ant, SD=0.27).
497 Hemolymph was collected from CO_2-anesthetized ants by puncturing the junction
498 between the foreleg and the distal edge of the thoracic plate with a pulled glass pipette. This
499 position was chosen over the abdomen in order to ensure that hemolymph was collected and
500 not the contents of the crop. Approximately 0.1 µl was taken from each ant.
501 Midgut samples were collected by first anesthetizing an ant, immobilizing it in warm wax
502 ventral-side up, covering the preparation in 1x PBS, and opening the abdomen with dissection
503 forceps and iris scissors. The midgut was punctured by a sharp glass pipette and its contents
504 collected. Because the pipette also contacts the surrounding fluid, some hemolymph
505 contamination was unavoidable.
506
507 **Proteomic analyses**

508 *Gel separation and protein digestion*

509 Protein samples were loaded on a 12% mini polyacrylamide gel and migrated about 2.5 cm.
510 After Coomassie staining, regions of gel lanes containing visible bands (generally > 18 kDa)
511 were excised into 2-4 pieces, depending on the gel pattern of considered experiment. Gel
512 pieces were digested with sequencing-grade trypsin (Promega) as described [116]. Extracted
513 tryptic peptides were dried and resuspended in 0.1% formic acid, 2% (v/v) acetonitrile for mass
514 spectrometry analyses.

515

516 *Proteomic mass spectrometry analyses*

517 Tryptic peptide mixtures were injected on a Dionex RSLC 3000 nanoHPLC system (Dionex,
518 Sunnyvale, CA, USA) interfaced via a nanospray source to a high resolution mass spectrometer
519 based on Orbitrap technology (Thermo Fisher, Bremen, Germany): LTQ-Orbitrap XL ('voluntary'
520 and hemolymph samples), LTQ-Orbitrap Velos (*A. mellifera* TF samples) or QExactive Plus
521 ('voluntary' and all other samples). Peptides were loaded onto a trapping microcolumn Acclaim
522 PepMap100 C18 (20 mm x 100 µm ID, 5 µm, Dionex) before separation on a C18 reversed-
523 phase analytical nanocolumn at a flowrate of 0.3 µL/min. Q-Exactive Plus instrument was
524 interfaced with an Easy Spray C18 PepMap nanocolumn (25 or 50 cm x 75µm ID, 2µm, 100Å,

Dionex) using a 35 min gradient from 4 to 76% acetonitrile in 0.1% formic acid for peptide separation (total time: 65 min). Full MS surveys were performed at a resolution of 70,000 scans. In data-dependent acquisition controlled by Xcalibur software (Thermo Fisher), the 10 most intense multiply charged precursor ions detected in the full MS survey scan were selected for higher energy collision-induced dissociation (HCD, normalized collision energy NCE=27%) and analyzed in the orbitrap at 17,500 resolution. The window for precursor isolation was of 1.6 *m/z* units around the precursor and selected fragments were excluded for 60 s from further analysis.

The LTQ-Orbitrap Velos mass spectrometer was interfaced with a reversed-phase C18 Acclaim Pepmap nanocolumn (75 µm ID x 25 cm, 2.0 µm, 100 Å, Dionex) using a 65 min gradient from 5 to 72% acetonitrile in 0.1% formic acid for peptide separation (total time: 95 min). Full MS surveys were performed at a resolution of 60,000 scans. In data-dependent acquisition controlled by Xcalibur software, the 20 most intense multiply charged precursor ions detected in the full MS survey scan were selected for CID fragmentation (NCE=35%) in the LTQ linear trap with an isolation window of 3.0 *m/z* and then dynamically excluded from further selection for 120 s.

LTQ-Orbitrap XL instrument was interfaced with a reversed-phase C18 Acclaim Pepmap (75 µm ID x 25 cm, 2.0 µm, 100 Å, Dionex) or Nikkyo (75 µm ID x 15 cm, 3.0 µm, 120Å, Nikkyo Technos, Tokyo, Japan) nanocolumn using a 90 min gradient from 4 to 76% acetonitrile in 0.1% formic acid for peptide separation (total time: 125 min). Full MS surveys were performed at a resolution of 60,000 scans. In data-dependent acquisition controlled by Xcalibur software, the 10 most intense multiply charged precursor ions detected in the full MS survey scan were selected for CID fragmentation (NCE=35%) in the LTQ linear trap with an isolation window of 4.0 *m/z* and then dynamically excluded from further selection for 60 s.

Proteomic data analysis

MS data were analyzed primarily using Mascot 2.5 (RRID:SCR_014322, Matrix Science, London, UK) set up to search either the UniProt (RRID:SCR_002380, www.uniprot.org) or NCBI (RRID:SCR_003496, www.ncbi.nlm.nih.gov) database restricted to *C. floridanus* (UniProt, August 2014 version: 14,801 sequences; NCBI, July 2015 version: 34,390 sequences), *S. invicta* (UniProt, August 2014 version: 14,374 sequences; NCBI, January 2015 version: 21,118 sequences) or *A. mellifera* (UniProt, September 2015 version: 15,323 sequences; NCBI, February 2016 version: 21,772 sequences) taxonomy. For Mascot search of *C. fellah* samples,

we used the database provided by the *C. fellah* transcriptome (27,062 sequences) and the UniProt *C. floridanus* reference proteome (January 2016 version, 14,287 sequences). Trypsin (cleavage at K, R) was used as the enzyme definition, allowing 2 missed cleavages. Mascot was searched with a parent ion tolerance of 10 ppm and a fragment ion mass tolerance of 0.50 Da (LTQ-Orbitrap Velos / LTQ-Orbitrap XL) or 0.02 Da (QExactive Plus). The iodoacetamide derivative of cysteine was specified in Mascot as a fixed modification. N-terminal acetylation of protein, deamidation of asparagine and glutamine, and oxidation of methionine were specified as variable modifications.

Scaffold software (version 4.4, RRID:SCR_014345, Proteome Software Inc., Portland, OR) was used to validate MS/MS based peptide and protein identifications, and to perform dataset alignment. Peptide identifications were accepted if they could be established at greater than 90.0% probability as specified by the Peptide Prophet algorithm [117] with Scaffold delta-mass correction. Protein identifications were accepted if they could be established at greater than 95.0% probability and contained at least two identified peptides. Protein probabilities were assigned by the Protein Prophet algorithm [118]. Proteins that contained similar peptides and could not be differentiated based on MS/MS analysis alone were grouped to satisfy the principles of parsimony and in most cases these proteins appear identical in annotations.

Quantitative spectral counting was performed using the normalized spectral abundance factor (NSAF), a measure that takes into account the number of spectra matched to each protein, the length of each protein and the total number of proteins in the input database [111]. To compare relative abundance across samples with notably different protein abundance, we divided each protein's NSAF value by the total sum of NSAF values present in the sample.

Across forced TF samples, ~10% of detected spectra were identified as peptides by Mascot and Scaffold, while in hemolymph samples ~16% of spectra were identified. Of those identified protein spectra in TF, about 2/3 mapped to the *C. floridanus* proteome, 1/3 to typical proteomic experiment contaminants (e.g., human keratin, trypsin added for digestion of proteins), < 5% to elements from the ants' diet (egg proteins, *D.melanogaster*), and <0.5% to microbial components including endosymbiont *Blochmannia floridanus.* Of the identified hemolymph protein spectra, 94% mapped to the *C. floridanus* proteome and the remaining 6% to keratins, trypsins, etc. We used PEAKS proteomic software (version 7.5, Bioinformatics Solutions Inc., Waterloo, Canada) for a more in-depth analysis of a typical TF sample, making less stringent *de novo* protein predictions allowing substitutions and post-translational modifications, and we could identify approximately 50% of spectra as peptides.

All proteomics data are available through ProteomeXchange at PXD004825.
Secretion signals were predicted using SignalP 4.1 [119].

Social isolation

Groups of 25-30 *C. floridanus* worker ants were taken from colonies C3, C6, C7, C8, C9 and C10 (queens all collected in the Florida Keys December 2012). Upon collection, TF was collected under CO_2 anesthesia. Immediately after TF collection ants were collectively isolated from their home colony and queen in fluon-coated plastic boxes with shelter, insect-free food (maple syrup, chicken eggs, tuna and agar), and water. Ants were kept in these group-isolated queenless conditions for 14 days. After 14 days, their TF was collected again.

Small RNA analysis

Total RNA isolation and quantification

Total RNA was isolated [120] from approximately 100 µL of TF from *C. floridanus* ants by the Trizol-LS™ method according to the manufacturer's protocols (Life Technologies, Inc., Grand Island, NY). A Qubit® RNA HS Assay Kit (high sensitivity, 5 to 100 ng) was used with a Qubit 3.0 fluorometer according to the manufacturer's protocols (Life Technologies, Carlsbad, USA); a sample volume of 1 µL was added to 199 µL of a Qubit working solution. The RNA concentration was 17.7 ng/µL.

Library preparation

We used 5 µL of RNA (approximately 88.5 ng) to generate a small RNA sequencing library using reagents and methods provided with TruSeq Small RNA Sample Prep Kit (Illumina, San Diego, USA). Briefly, T4 RNA ligase was used to ligate RA5 and RA3 RNA oligonucleotides to 5' and 3' ends of RNA, respectively. Adapter-ligated RNA was reverse-transcribed using a RTP primer and the resulting cDNA was amplified in an 11-cycle PCR that used RP1 and indexed RP1 primers. We size-selected cDNA libraries using 6% TBE PAGE gels (Life Technologies) and ethidium bromide staining. Quality of the generated small RNA sequencing library was confirmed using electropherograms from a 2200 TapeStation System (Agilent Technologies, Santa Clara, CA). Desired sizes of cDNA bands were cut from the gel (between 147 and 157 nt), the gel matrix broken by centrifugation through gel breaker tubes (IST Engineering Inc.), and cDNA eluted with 400 µL of 0.3M Na-Chloride. Further purification of cDNA was by centrifugation through Spin-X 0.22µm cellulose acetate filter columns (Costar) followed by

ethanol precipitation. Libraries were sequenced on a HiSeq 2000 Sequencer (Illumina). Small RNA sequencing data are available through SRA database at SRP082161.

Pre-processing of RNA libraries

Raw sequenced reads from small RNA libraries were submitted to quality filtering and adaptor trimming using cutadapt (version 1.8.1, RRID:SCR_011841, https://pypi.python.org/pypi/cutadapt/1.8.1). Small RNA reads with Phred quality below 20, and fewer than 18 nucleotides after trimming of adaptors, were discarded.

MicroRNA prediction using miRDeep2

Remaining sequences from small RNA libraries were used with *A. melifera* microRNA database (miRbase version 21) and *C. floridanus* genome (NCBI version 1.0) to predict microRNAs precursors using miRDeep2 (RRID:SCR_012960) with default parameters and GFF (General Feature Format) file extracted by perl scripts.

Small RNA reads mapped to C. floridanus and D. melanogaster genomes

Approximately half the reads that mapped to the *C. floridanus* genome also mapped to *D. melanogaster,* a component of the ants' lab diet. While some of these RNAs are likely to be endogenous *C. floridanus* RNAs, we eliminated all reads identical between *C. floridanus* and *D. melanogaster.* Remaining sequences from small RNA libraries were mapped to reference sequences from *C. floridanus* and *D. melanogaster* genomes using Bowtie (version 1.1.1, RRID:SCR_005476, one mismatch allowed). The *C. floridanus* genome (version 1.0) was downloaded from NCBI. The *D. melanogaster* genome (version v5.44) was downloaded from flybase.org. Remaining sequenced reads that did not map to the *C. floridanus* or *D. melanogaster* genome were assembled into contigs with VelvetOptimiser (version 2.2.5; http://bioinformatics.net.au/software.velvetoptimiser.shtml), and BLASTed against non-redundant NCBI bacteria and viruses databases to assess their source organism. Hits with an E-value smaller than 1e−5 for nucleotide comparison were considered significant.

Automatic annotation, penalization, size distribution and gene expression

To perform automatic annotation we used BedTools (version v2.17.0, RRID:SCR_006646) to compare genomic coordinates from mapped reads against predicted microRNAs, mRNA, tRNA and ncRNA (represented by lncRNA). Reads mapping to both the *C. floridanus* and *D. melanogaster* genomes were deemed ambiguous and were eliminated. The remaining reads

were normalized by reads per million (RPM). The gene expression was measured and normalized by RPM and plotted in heatmap and barplot graphs.

Gas chromatography mass spectrometry and related sample preparation

Hydrocarbon analysis was performed on trophallactic fluid from five groups of 20-38 ants, each collected from one of five different colonies (C11-C15). TF samples were placed directly into 3:1 hexane:methanol. Immediately after TF collection, body surface CHCs were collected by placing anesthetized ants in hexane for one minute before removal with cleaned forceps. Methanol was added to the cuticular-extraction hexane (maintaining the 3:1 proportion of the TF samples). The TF and body samples were vortexed for 30 s and centrifuged for 7 min. Hexane fractions were collected using a thrice-washed Hamilton syringe. Samples were kept at -20°C until further analysis.

A Trace 1300 GC chromatograph interfaced with a TSQ 8000 Evo Triple Quadrupole Mass Spectrometer (Thermo Scientific, Bremen, Germany) was used for the study. Hydrocarbons were separated on a 30 m x 0.25 mm I.D. (0.25 mm film thickness) Zebron ZB-5 ms capillary column (Phenomenex) using the following program: initial temperature 70°C held for 1 min, ramped to 210°C at 8°C/min, ramped to 250 °C at 2 °C/min, ramped to 300°C at 8°C/min and held for 5 min. Helium was used as carrier gas at a constant flow of 1 mL/min. Injections of 1 µL of ants' TF or body extracts were made using splitless mode. The injection port and transfer line temperature were kept at 250°C, and the ion source temperature set at 200°C. Ionization was done by electron-impact (EI, 70 eV) and acquisition performed in full scan mode in the mass range 50-550 *m/z* (scan time 0.2 sec). Identification of hydrocarbons was done using XCalibur and NIST 14 library. The TIC MS was integrated and the area reported as a function of Retention time (Rt, min) for each peak.

Identification of trophallactic fluid hydrocarbons

Characterization of branched alkanes by GC-MS remains a challenge due to the similarity of their electron impact (EI) mass spectra and the paucity of corresponding spectra listed in EI mass spectra databases. A typical GC-MS chromatogram (Figure 3-figure supplement 1A) reveals the complexity of the TF sample. The workflow described here was systematically used to characterize the linear and branched hydrocarbons present in TF samples summarized in Table 1. The parent ion was first determined for each peak after background subtraction. Ambiguities remained in some cases due to the low intensity or absence of the molecular ion. In

order to determine the number of ramifications for alkanes and alkenes we examined the distribution of intensities of all fragment ions in the spectrum. From the experimental mass spectrum (Figure 3-figure supplement 1B-C), the intensity of all fragment ions was extracted and fitted with an exponential decay function (Figure 3-figure supplement 1D-E). Figure 3-figure supplement 1 clearly shows two different resulting EI mass spectra profiles: on the left a linear alkane corresponding to n-hexacosane (Rt=34.69 min and MF $C_{26}H_{54}$); on the right, a ramified structure most likely corresponding to 9,20-Dimethyl nonacosane (Rt=43.29 min and MF $C_{31}H_{64}$) with fragment ions 141 (loss of 295) and 309 (loss of 127) from the molecular ion at *m/z* 436. This demonstrates that extracting and fitting the fragment profile provides a reliable method, not only to discriminate between linear and branched hydrocarbons, but also to determine the number of ramifications. Once the number of ramifications and the parent ion mass were known, the position of the different ramifications could be deduced.

To determine the positions of the ramifications we next estimated the Kovats retention index (RI) for each proposed structure. Since most branched alkanes are not present in the main libraries of EI mass spectra, a predicted RI was determined depending on: i) the number of carbons and ii) the number of ramifications. Based on RI values (for similar GC stationary phase) given in the NIST Chemistry WebBook [121] for known alkanes from C15 to C38, 6 different curves of RI vs. number of carbons were constructed for each class of alkane, from linear to pentamethylated alkanes (Figure 3-figure supplement 1F). For the same number of carbons and ramifications, an average value of RI was calculated. For example, the RI value given for $C_{25}H_{52}$ and two ramifications (RI=2409) is the average of 3,(7/9/11/13)-dimethyltricosane (RI=2405), 3,(3/5)-dimethyltricosane (RI=2444) and 5,(9/11)-dimethyltricosane (RI=2380) values listed in the NIST Chemistry WebBook. The curve corresponding to linear alkanes was strictly superimposed with the one obtained in our conditions with a standard mixture of C8-C40 alkanes. Those curves were used to determine RI values for all proposed hydrocarbons in TF samples.

As a final validation for the class of hydrocarbon proposed, the experimental retention time of each compound was plotted as a function of the calculated RI index (Figure 3-figure supplement 1G). The experimental plot was overlaid with values we recorded for linear alkane standards C8-C40. For each proposed hydrocarbon, the Kovats index should fit this curve. The table in Table 1 summarizes all the proposed structures for hydrocarbons and other compounds detected in TF samples.

JH quantification by GC-MS

For each sample, a known quantity of TF or hemolymph was collected into a graduated glass capillary tube and blown into an individual glass vial containing 5 µl of 100% ethanol. Samples were kept at -20ºC until further processing. This biological sample was added to a 1:1 mixture of isooctane and methanol, vortexed for 30 sec, and centrifuged for 7 min at maximum speed. Avoiding the boundary between phases, the majority of the isooctane layer and the methanol layer were removed separately, combined and stored at –80ºC until analysis. Before analysis, 50% acetonitrile (HPLC grade) was added. Prior to purification, farnesol (Sigma-Aldrich, St Louis, MO, U.S.A.) was added to each sample to serve as an internal standard. Samples were extracted three times with hexane (HPLC grade). The hexane fractions were recombined in a clean borosilicate glass vial and dried by vacuum centrifugation. JH III was quantified using the gas chromatography mass spectrometry (GC–MS) method of [59] as modified by [58] and [57]. The residue was washed out of the vials with three rinses of hexane and added to borosilicate glass columns filled with aluminum oxide. In order to filter out contaminants, samples were eluted through the columns successively with hexane, 10% ethyl ether–hexane and 30% ethyl ether–hexane. After drying, samples were derivatized by heating at 60°C for 20 min in a solution of methyl-d alcohol (Sigma-Aldrich) and trifluoroacetic acid (Sigma-Aldrich, St Louis, MO, U.S.A.). Samples were dried down, resuspended in hexane, and again eluted through aluminum oxide columns. Non-derivatized components were removed with 30% ethyl ether. The JH derivative was collected into new vials by addition of 50% ethyl-acetate–hexane. After drying, the sample was resuspended in hexane. Samples were then analyzed using an HP 7890A Series GC (Agilent Technologies, Santa Clara, CA, U.S.A.) equipped with a 30 m x 0.25 mm Zebron ZB-WAX column (Phenomenex, Torrence, CA, U.S.A.) coupled to an HP 5975C inert mass selective detector. Helium was used as a carrier gas. JH form was confirmed by first running test samples in SCAN mode for known signatures of JH 0, JH I, JH II, JH III and JH III ethyl; JH III was confirmed as the primary endogenous form in this species. Subsequent samples were analyzed using the MS SIM mode, monitoring at m/z 76 and 225 to ensure specificity for the d_3-methoxyhydrin derivative of JH III. Total abundance was quantified against a standard curve of derivatized JH III, and adjusted for the starting volume of TF. The detection limit of the assay is approximately 1 pg.

Long-term development

To determine the effect of exogenous JH on larval development, ants were taken from laboratory *C. floridanus* colonies (Expt 1: C2, C3, C5, C9, C16, C17; Expt 2: C4, C5, C6, C18; Expt 3: C1, C5, C6, C7, C11, C16, C19). Approximately 90% of the ants were taken from inside

the nest on the brood, while the remaining 10% were taken from outside the nest. Each colony explant had 20-30 workers (each treatment had the same number of replicates of any given colony) and was provided with five to ten 2nd or 3rd instar larvae from their own colony of origin (staged larvae were equally distributed across replicates). Each explant was provided with water, and either solvent- or JH III-supplemented 30% sugar water and maple-syrup-based ant diet (1500 ng of JH III in 5 µl of ethanol was applied to each 3x3x3 mm food cube and sucrose solution had 83 ng JH III/µl). No insect-based food was provided. Food sources were refreshed twice per week. JH was found to transition to JH acid gradually at room temperature, where after one week ~ 50% was JH acid (as measured by radio-assay as in [122], data not shown).

Twice weekly before feeding, each explant was checked for pupae, and developing larvae were measured and counts using a micrometer in the reticle of a stereomicroscope. Upon pupation, or cocoon spinning, larvae/pupae were removed from the care of workers and kept in a clean humid chamber until metamorphosis. Cocoons were removed using dissection forceps. The head width of the pupae was measured using a micrometer in the reticle of a stereomicroscope 1-4 days after metamorphosis (immediately after removal of the larval sheath, head width is not stable). Long-term development experiments were stopped when fewer than three larvae remained across all explants and these larvae had not changed in size for two weeks. Of larvae that did not successfully undergo metamorphosis, approximately 75% were eaten by nursing workers at varying developmental stages over the course of the experiment. The remaining non-surviving larvae were split between larvae that finished the cocoon spinning phase [123] but did not complete metamorphosis and larvae that had ceased to grow by the end of the approximately 10-week experiment.

C. fellah transcriptomics

Transcriptome sequencing

We sequenced the *C. fellah* transcriptome (RNAseq) of workers from a single colony initiated from a queen collected during a mating flight in 2007 in Tel Aviv, Israel. Total RNA was extracted from the whole body of four minor workers with RNeasy Plus micro kit and RNase-Free DNase Set (QIAGEN) and then 350 ng cDNA from each ant were pooled and sequenced. Illumina cDNA library was constructed and sequenced using strand-specific, paired-end sequencing of 100 bp reads. The library was sequenced on an Illumina HiSeq machine, which generated a total of 115 million pairs of reads.

Transcriptome assembly

We ran Trinity [124] (version r2013-02-25, RRID:SCR_013048) on these sequence reads to assemble the *C. fellah* transcriptome. Reads were filtered according to the Illumina Chastity filter and then trimmed and filtered using Trimmomatic [125] (RRID:SCR_011848, parameters: ILLUMINACLIP:TruSeq3-PE.fa:2:30:10 SLIDINGWINDOW:4:15 MINLEN:50). Trinity was run with default parameters for strand-specific, paired-read data. The assembled transcriptome consists of 66, 156 genes ("components") with 99, 402 transcripts, with putative open reading frames found in 9,987 and 27,062 of them, respectively. The total sequence length is 109,526,661 bases (including alternative splice variants) and the N50 size is 2,243 bases. The *C. fellah* transcriptome dataset is available under accession number PRJNA339034.

Protein orthology

In order to identify orthologous proteins across the species TF, we first needed to determine orthology across the four species. Compiling RefSeq, UniProt, and transcriptome protein models from the four species yielded 131,122 predicted protein sequences. For *C. floridanus, A. mellifera* and *S. invicta*, this was done for both NCBI RefSeq and UniProt databases because there are discrepancies in annotation and thus in protein identification between databases. We determined 21,836 groups of one-to-one orthologs using OMA stand-alone [126] v.1.0.3, RRID:SCR_011978, though only 4,538 orthologous groups had members in all four species. Default parameters were used with the exception of minimum sequence length, which was lowered to 30 aa.

The 40 proteins with the highest average NSAF value across TF samples of that species were selected. For each of the top proteins, we checked across the other species and databases for orthologous proteins. If an orthologous protein was identified in the proteome, we then checked if that protein was also present in that species' TF, even at low abundance.

Dendrogram

The protein sequences of our proteomically identified TF *C. floridanus* JHE/Est-6 proteins, functionally validated JHEs (*Tribolium castaneum* JHE (UniProt D7US45), *A. mellifera* JHE (Q76LA5), *Manduca sexta* JHE (Q9GPG0), *D. melanogaster* JHE (A1ZA98) and *Culex quinquefasciatus* (R4HZP1) and Est-6 proteins from *A. mellifera* (B2D0J5) and *D. melanogaster* (P08171) were aligned using PROMALS3D with the crystal structure of the *M. sexta* JHE (2fj0) used as a functional guide. Phylogeny was inferred using Randomized Axelerated Maximum Likelihood (RAxML, RRID:SCR_006086 [127]), with 100 bootstrapped trees. The dendrogram was visualized in FigTree (v1.4.2, RRID:SCR_008515).

828

829 **Sample Sizes, Data Visualization and Statistics**

830 The proteomic sample sizes were determined by the variation observed in protein IDs and
831 abundances in unmanipulated samples. Visualization together with hierarchical clustering was
832 done in R version 3.0.2 (www.r-project.org, RRID:SCR_001905) using the 'heatmap.3' package
833 in combination with the pvclust package. Heatmap visualization without clustering was done in
834 MATLAB (2012b, RRID:SCR_001622). For experiments in Figures 3 and 4, the number of
835 colonies and number of replicates or ants per colony were determined by both preliminary trials
836 to assess sample variation and the health/abundance of the *C. floridanus* ant colonies available
837 in the lab. Hydrocarbon GC-MS traces were analyzed in MATLAB normalizing the abundance
838 (area under curve) of each point by maximum and minimum value within the CHC retention time
839 window. Peaks were found using 'findpeaks' with a lower threshold abundance of 7% of the total
840 abundance for that sample. To compare across samples, peaks were filtering into 0.03 min bins
841 by retention time. Cross-correlation was computed using the 'xcorr' function. For long-term
842 development experiments, the number of same-staged larvae per colony was the limiting factor
843 for the number of replicates per experiment. Because of this limitation, the long-term
844 development experiment testing the effect of JH was fully repeated three times. Colonies were
845 hibernated approximately one month prior to each of these experiments to maximize number of
846 same-staged brood. General linear mixed models (GLMM) were used so that colony, replicate
847 and experiment could be considered as random factors. Models were done in R using 'lmer' and
848 'glmer' functions of the lme4 package, and *p* values were calculated with the 'lmerTest' package
849 in R. Overall no data points were excluded as outliers and all replicates discussed are biological
850 not technical replicates.

851

Acknowledgements

We thank Robert I'Anson Price and Thomas Richardson for access to *A. mellifera* colonies, and Raphaël Braunschweig for access to *C. fellah* colonies. We thank George Shizuo Kamita for advice on JHEs. This work was funded by an ERC Advanced Grant (249375) and a Swiss NSF grant to L.K., an ERC Starting Independent Researcher and Consolidator Grants (205202 and 615094) and a Swiss NSF Grant to R.B. Mention of trade names or commercial products in this article is solely for the purpose of providing specific information and does not imply recommendation or endorsement by the U.S. Department of Agriculture. USDA is an equal opportunity provider and employer. Z.S.G. was supported by CAPES Brazil. E.A.M. was supported by Wellcome Trust (104640/Z/14/Z). We would like to thank Sylviane Moss and Kay Harnish for help with high-throughput sequencing and Alexandra Bezler, Thomas Auer, Roman Arguello, Juan Alcaniz-Sanchez, Pavan Ramdya, Lucia Prieto-Godino, Katja Hoedjes, Raphaël Braunschweig and Sean McGregor for their useful comments on the manuscript.

Author Contributions

ACL managed the project and did all sample collection, isolation and long-term development experiments, data analysis, and figure production. RB and LK oversaw and directed the project. ACL, RB and LK wrote the manuscript.

PW performed proteomic LC-MS/MS for all samples. CSB performed GC-MS for Fig. 4A and B and LM and DO performed GC-MS and molecule identification for Fig. 3. ORG performed expression analysis. AK performed the RNA preparation and EP performed assembly and annotation of the *C. fellah* transcriptome. ZGS performed RNA extraction and library preparation for small RNA library, ANG performed small RNA bioinformatics analyses. EAM designed the small RNA sequencing experiments.

References

1. Poiani A. Complexity of seminal fluid: A review. Behav Ecol Sociobiol. 2006;60: 289–310. doi:10.1007/s00265-006-0178-0
2. Liu HF, Kubli E. Sex-peptide is the molecular basis of the sperm effect in Drosophila melanogaster. Proc Natl Acad Sci U S A. 2003;100: 9929–9933. doi:10.1073/pnas.1631700100
3. Liu B, Zupan B, Laird E, Klein S, Gleason G, Bozinoski M, et al. Maternal hematopoietic TNF, via milk chemokines, programs hippocampal development and memory. Nat Neurosci. Nature Publishing Group; 2014;17: 97–105. doi:10.1038/nn.3596

4. Bernt KM, Walker WA. Human milk as a carrier of biochemical messages. Acta Paediatr Suppl. 1999;88: 27–41. doi:10.1111/j.1651-2227.1999.tb01298.x
5. Perry JC, Sirot L, Wigby S. The seminal symphony: How to compose an ejaculate. Trends Ecol Evol. Elsevier Ltd; 2013;28: 414–422. doi:10.1016/j.tree.2013.03.005
6. Bonabeau E, Theraulaz G, Deneubourg JL, Aron S, Camazine S. Self-organization in social insects. Trends in Ecology and Evolution. 1997. pp. 188–193. doi:10.1016/S0169-5347(97)01048-3
7. LeBoeuf AC, Grozinger CM. Me and we: the interplay between individual and group behavioral variation in social collectives. Curr Opin Insect Sci. 2014; doi:10.1016/j.cois.2014.09.010
8. Hölldobler B, Wilson EO. The Ants. Harvard University Press. 1990.
9. Boulay R, Hefetz A, Soroker V, Lenoir A. Camponotus fellah colony integration: worker individuality necessitates frequent hydrocarbon exchanges. Anim Behav. 2000;59: 1127–1133. doi:10.1006/anbe.2000.1408
10. Greenwald E, Segre E, Feinerman O. Ant trophallactic networks: simultaneous measurement of interaction patterns and food dissemination. Sci Rep. 2015;5: 12496. doi:10.1038/srep12496
11. Malcolm JR, Marten K. Natural selection and the communal rearing of pups in African wild dogs (*Lycaon pictus*). Behav Ecol Sociobiol. 1982;10: 1–13. doi:10.1007/BF00296390
12. Wilkinson GS. Reciprocal food sharing in the vampire bat. Nature. 1984;308: 181–184. doi:10.1038/308181a0
13. Wilson EO, Eisner T. Quantitative studies of liquid food transmission in ants. Insectes Soc. 1957;4: 157–166. doi:10.1007/BF02224149
14. Buffin A, Denis D, Van Simaeys G, Goldman S, Deneubourg JL. Feeding and stocking up: Radio-labelled food reveals exchange patterns in ants. PLoS One. 2009;4. doi:10.1371/journal.pone.0005919
15. Cassill DL, Tschinkel WR. A duration constant for worker-to-larva trophallaxis in fire ants. Insectes Soc. 1996;43: 149–166. doi:10.1007/BF01242567
16. Cassill DL, Tschinkel WR. Allocation of liquid food to larvae via trophallaxis in colonies of the fire ant, *Solenopsis invicta*. Anim Behav. 1995;50: 801–813. doi:10.1016/0003-3472(95)80140-5
17. Wheeler WM. A study of some ant larvae, with a consideration of the origin and meaning of the social habit among insects. Proc Amer Phil Soc. 1918;57: 293–339.

18. Wheeler DE. Developmental and Physiological Determinants of Caste in Social Hymenoptera : Evolutionary Implications. Am Nat. 1986;128: 13–34.
19. Terra WR. Evolution of Digestive Systems of Insects: Compartmentalization of the Digestive Process. 1990; 181–200.
20. Eisner T, Brown WLJ. The evolution and social significance of the ant proventriculus. Proceedings Tenth International Congress of Entomology. 1958. pp. 503–508.
21. Lanan MC, Rodrigues PAP, Agellon A, Jansma P, Wheeler DE. A bacterial filter protects and structures the gut microbiome of an insect. ISME J. Nature Publishing Group; 2016; 1–11. doi:10.1038/ismej.2015.264
22. Hunt JH. Nourishment and the evolution of the social Vespidae. The social biology of wasps. 1991. pp. 426–450.
23. Grüter C, Acosta LE, Farina WM. Propagation of olfactory information within the honeybee hive. Behav Ecol Sociobiol. 2006;60: 707–715. doi:10.1007/s00265-006-0214-0
24. Farina WM, Grüter C, Acosta L, Mc Cabe S. Honeybees learn floral odors while receiving nectar from foragers within the hive. Naturwissenschaften. 2007;94: 55–60. doi:10.1007/s00114-006-0157-3
25. Boulay R, Soroker V, Godzinska EJ, Hefetz A, Lenoir A. Octopamine reverses the isolation-induced increase in trophallaxis in the carpenter ant Camponotus fellah. J Exp Biol. 2000;203: 513–520.
26. Hamilton C, Lejeune BT, Rosengaus RB. Trophallaxis and prophylaxis: social immunity in the carpenter ant *Camponotus pennsylvanicus*. Biol Lett. 2011;7: 89–92. doi:10.1098/rsbl.2010.0466
27. Liebig J, Heinze J, Hölldobler B. Trophallaxis and aggression in the ponerine ant, Ponera coarctata: implications for the evolution of liquid food exchange in the Hymenoptera. Ethology. 1997;103: 707–722. doi:10.1111/j.1439-0310.1997.tb00180.x
28. Soroker V, Vienne C, Hefetz A. Hydrocarbon Dynamics Within and Between Nestmates In Cataglyphis-niger (hymenoptera, Formicidae). J Chem Ecol. 1995;21: 365–378. doi:10.1007/BF02036724
29. Bonasio R, Zhang G, Ye C, Mutti NS, Fang X, Qin N, et al. Genomic Comparison of the Ants *Camponotus floridanus* and *Harpegnathos saltator*. Science. 2010;329: 1068–1071. doi:10.1126/science.1192428
30. Dahbi A, Hefetz A, Cerda X, Lenoir A. Trophallaxis mediates uniformity of colony odor in *Cataglyphis iberica* ants (Hymenoptera, Formicidae). J Insect Behav. 1999;12: 559–567.

954 doi:10.1023/A:1020975009450
955 31. Zhou X, Tarver MR, Scharf ME. Hexamerin-based regulation of juvenile hormone-
956 dependent gene expression underlies phenotypic plasticity in a social insect.
957 Development. 2007;134: 601–610. doi:10.1242/dev.02755
958 32. Drapeau MD, Albert S, Kucharski R, Prusko C, Maleszka R. Evolution of the Yellow /
959 Major Royal Jelly Protein family and the emergence of social behavior in honey bees.
960 Genome Res. 2006; 1385–1394. doi:10.1101/gr.5012006.
961 33. Kutty RK, Kutty G, Kambadur R, Duncan T, Koonin E V., Rodriguez IR, et al. Molecular
962 characterization and developmental expression of a retinoid- and fatty acid-binding
963 glycoprotein from Drosophila. A putative lipophorin. J Biol Chem. 1996;271: 20641–
964 20649. doi:10.1074/jbc.271.34.20641
965 34. Kamita SG, Hammock BD. Juvenile hormone esterase: biochemistry and structure. J
966 Pestic Sci. 2010;35: 265–274. doi:10.1584/jpestics.R10-09
967 35. Nijhout HF, Riddiford LM, Mirth C, Shingleton AW, Suzuki Y, Callier V. The
968 developmental control of size in insects. Wiley Interdiscip Rev Dev Biol. 2014;3: 113–134.
969 doi:10.1002/wdev.124
970 36. Mane SD, Tompkins L, Richmond RC. Male Esterase 6 Catalyzes the Synthesis of a Sex
971 Pheromone in Drosophila melanogaster Females. Science. 1983;222: 419–21.
972 doi:10.1126/science.222.4622.419
973 37. Richmond RC, Gilbert DG, Sheehan KB, Gromko MH, Butterworth FM. Esterase 6 and
974 reproduction in Drosophila melanogaster. Science. 1980;207: 1483–5.
975 doi:10.1126/science.6767273
976 38. Younus F, Chertemps T, Pearce SL, Pandey G, Bozzolan F, Coppin CW, et al.
977 Identification of candidate odorant degrading gene/enzyme systems in the antennal
978 transcriptome of Drosophila melanogaster. Insect Biochem Mol Biol. 2014;53: 30–43.
979 doi:10.1016/j.ibmb.2014.07.003
980 39. Qu Z, Kenny NJ ames, Lam HM ing, Chan TF ung, Chu KH ou, Bendena WG, et al. How
981 Did Arthropod Sesquiterpenoids and Ecdysteroids Arise? Comparison of Hormonal
982 Pathway Genes in Noninsect Arthropod Genomes. Genome Biol Evol. 2015;7: 1951–
983 1959. doi:10.1093/gbe/evv120
984 40. Sarkies P, Miska EA. Is there social RNA? Science. 2013;341: 467–468.
985 doi:10.1126/science.1243175
986 41. Weber JA, Baxter DH, Zhang S, Huang DY, Huang KH, Lee MJ, et al. The microRNA
987 spectrum in 12 body fluids. Clin Chem. 2010;56: 1733–1741.

doi:10.1373/clinchem.2010.147405

42. Guo X, Su S, Skogerboe G, Dai S, Li W, Li Z, et al. Recipe for a busy bee: MicroRNAs in honey bee caste determination. PLoS One. 2013;8. doi:10.1371/journal.pone.0081661

43. Turchinovich A, Weiz L, Burwinkel B. Extracellular miRNAs: The mystery of their origin and function. Trends Biochem Sci. Elsevier Ltd; 2012;37: 460–465. doi:10.1016/j.tibs.2012.08.003

44. Søvik E, Bloch G, Ben-Shahar Y. Function and evolution of microRNAs in eusocial Hymenoptera. Front Genet. 2015;6: 193. doi:10.3389/fgene.2015.00193

45. Greenberg JK, Xia J, Zhou X, Thatcher SR, Gu X, Ament S a, et al. Behavioral plasticity in honey bees is associated with differences in brain microRNA transcriptome. Genes Brain Behav. 2012;11: 660–70. doi:10.1111/j.1601-183X.2012.00782.x

46. Kaewkascholkul N, Somboonviwat K, Asakawa S, Hirono I, Tassanakajon A, Somboonwiwat K. Shrimp miRNAs regulate innate immune response against white spot syndrome virus infection. Dev Comp Immunol. Elsevier Ltd; 2016;60: 191–201. doi:10.1016/j.dci.2016.03.002

47. Crozier RH, Dix MW. Analysis of two genetic models for the innate components of colony odor in social Hymenoptera. Behav Ecol Sociobiol. 1979;4: 217–224. doi:10.1007/BF00297645

48. Sharma KR, Enzmann BL, Schmidt Y, Moore D, Jones GR, Parker J, et al. Cuticular Hydrocarbon Pheromones for Social Behavior and Their Coding in the Ant Antenna. Cell Rep. 2015;12: 1261–71. doi:10.1016/j.celrep.2015.07.031

49. Bos N, Grinsted L, Holman L. Wax on, wax off: Nest soil facilitates indirect transfer of recognition cues between ant nestmates. PLoS One. 2011;6. doi:10.1371/journal.pone.0019435

50. Hefetz A. The evolution of hydrocarbon pheromone parsimony in ants (Hymenoptera : Formicidae) – interplay of colony odor uniformity and odor idiosyncrasy . A review. Regulation. 2007;10: 59–68.

51. Lahav S, Soroker V, Hefetz A, Vander Meer RK. Direct behavioral evidence for hydrocarbons as ant recognition discriminators. Naturwissenschaften. 1999;86: 246–249. doi:10.1007/s001140050609

52. Ozaki M, Wada-Katsumata A, Fujikawa K, Iwasaki M, Yokohari F, Satoji Y, et al. Ant Nestmate and Non-Nestmate Discrimination by a Chemosensory Sensillum. Science. 2005;309: 311–314. doi:10.1126/science.1105244

53. van Zweden JS, d'Ettorre P. Nestmate recognition in social insects and the role of

hydrocarbons. Insect Hydrocarb Biol Biochem Chem Ecol. 2010; 222–243. doi:10.1017/CBO9780511711909.012

54. Boulay R, Lenoir A. Social isolation of mature workers affects nestmate recognition in the ant Camponotus fellah. Behav Processes. 2001;55: 67–73. doi:10.1016/S0376-6357(01)00163-2

55. Endler A, Liebig J, Schmitt T, Parker JE, Jones GR, Schreier P, et al. Surface hydrocarbons of queen eggs regulate worker reproduction in a social insect. Proc Natl Acad Sci U S A. 2004;101: 2945–2950. doi:10.1073/pnas.0308447101

56. Wigglesworth VB. The function of the Corpus Allatum in the Growth and Reproduction of Rhodnius Prolixus (Hemiptera). Q J Microsc Sci. 1936;79: 91–121.

57. Brent CS, Vargo EL. Changes in juvenile hormone biosynthetic rate and whole body content in maturing virgin queens of Solenopsis invicta. J Insect Physiol. 2003;49: 967–974. doi:10.1016/S0022-1910(03)00166-5

58. Shu S, Ihl Park Y, Ramaswamy SB, Srinivasan A. Hemolymph juvenile hormone titers in pupal and adult stages of southwestern corn borer [*Diatraea grandiosella (pyralidae*)] and relationship with egg development. J Insect Physiol. 1997;43: 719–726. doi:10.1016/S0022-1910(97)00048-6

59. Bergot BJ, Ratcliff M, Schooley DA. Method for quantitative determination of the four known juvenile hormones in insect tissue using gas chromatography-mass spectroscopy. J Chromatogr A. 1981;204: 231–244. doi:10.1016/S0021-9673(00)81664-7

60. Nijhout HF, Wheeler DE. Juvenile Hormone and the Physiological Basis of Insect Polymorphisms. Q Rev Biol. 1982;57: 109–133.

61. Libbrecht R, Corona M, Wende F, Azevedo DO, Serrão JE, Keller L. Interplay between insulin signaling, juvenile hormone, and vitellogenin regulates maternal effects on polyphenism in ants. Proc Natl Acad Sci U S A. 2013;110: 11050–5. doi:10.1073/pnas.1221781110

62. Wheeler DE, Nijhout HF. Soldier Determination in Ants : New Role for Juvenile Hormone Soldier Determination in Ants : New Role for Juvenile Hormone. Science. 1981;213: 361–363.

63. Bacco A Di, Gill G. The secreted glycoprotein CREG inhibits cell growth dependent on the mannose-6-phosphate / insulin-like growth factor II receptor. Oncogene. 2003;22: 5436–5445. doi:10.1038/sj.onc.1206670

64. Li Y, Zhang Z, Robinson GE, Palli SR. Identification and Characterization of a Juvenile Hormone Response Element and Its Binding Proteins. Journal of Biological Chemistry.

2007; doi:10.1074/jbc.M704595200

65. Barchuk AR, Cristino AS, Kucharski R, Costa LF, Simões ZLP, Maleszka R. Molecular determinants of caste differentiation in the highly eusocial honeybee Apis mellifera. BMC Dev Biol. 2007;19: 1–19. doi:10.1186/1471-213X-7-70

66. Zhang L, Han B, Li R, Lu X, Nie A, Guo L, et al. Comprehensive identification of novel proteins and N-glycosylation sites in royal jelly. 2014; 1–14.

67. Kamakura M. Royalactin induces queen differentiation in honeybees. Nature. 2011;473: 478–483. doi:10.1038/nature10093

68. Huang X, Warren JT, Buchanan J, Gilbert LI, Scott MP. Drosophila Niemann-Pick type C-2 genes control sterol homeostasis and steroid biosynthesis: a model of human neurodegenerative disease. Development. 2007;134: 3733–3742. doi:10.1242/dev.004572

69. Humphrey SP, Williamson RT. A review of saliva: Normal composition, flow, and function. Journal of Prosthetic Dentistry. 2001. pp. 162–169. doi:10.1067/mpr.2001.113778

70. Ribeiro JMC. Insect Saliva: Function, Biochemistry, and Physiology. In: R. F. Chapman • Gerrit de Boer, editor. Regulatory Mechanisms in Insect Feeding. Chapman & Hall; 1995. pp. 74–97.

71. Soroker V, Vienne C, Hefetz A. Hydrocarbon dynamics within and between nestmates in *Cataglyphis niger* (Hymenoptera: Formicidae). J Chem Ecol. 1995;21: 365–78. doi:10.1007/BF02036724

72. Lalzar I, Simon T, Meer RK V, Hefetz A. Alteration of cuticular hydrocarbon composition affects heterospecific nestmate recognition in the carpenter ant Camponotus fellah. Chemoecology. 2010;20: 19–24. doi:10.1007/s00049-009-0030-x

73. Lemaitre B, Hoffmann J. The host defense of Drosophila melanogaster. Annu Rev Immunol. 2007;25: 697–743. doi:10.1146/annurev.immunol.25.022106.141615

74. Söderhäll K, Cerenius L. Role of the prophenoloxidase-activating system in invertebrate immunity. Current Opinion in Immunology. 1998. pp. 23–28. doi:10.1016/S0952-7915(98)80026-5

75. Saikhedkar N, Summanwar A, Joshi R, Giri A. Cathepsins of lepidopteran insects: Aspects and prospects. Insect Biochemistry and Molecular Biology. 2015. pp. 51–59. doi:10.1016/j.ibmb.2015.07.005

76. Ahn JE, Zhu-Salzman K. CmCatD, a cathepsin D-like protease has a potential role in insect defense against a phytocystatin. J Insect Physiol. 2009;55: 678–685. doi:10.1016/j.jinsphys.2009.04.016

77. Lucas A, Liu L, Dai E, Bot I, Viswanathan K, Munuswamy-Ramunujam G, et al. The serpin saga; development of a new class of virus derived anti-inflammatory protein immunotherapeutics. Adv Exp Med Biol. 2009;666: 132–156. doi:10.1007/978-1-4419-1601-3_11

78. Robb CT, Dyrynda EA, Gray RD, Rossi AG, Smith VJ. Invertebrate extracellular phagocyte traps show that chromatin is an ancient defence weapon. Nat Commun. 2014;5: 4627. doi:10.1038/ncomms5627

79. Brinkmann V, Reichard U, Goosmann C, Fauler B, Uhlemann Y, Weiss DS, et al. Neutrophil extracellular traps kill bacteria. Science. 2004;303: 1532–1535. doi:10.1126/science.1092385

80. Cnaani J, Borst DW, Huang ZY, Robinson GE, Hefetz A. Caste determination in *Bombus terrestris*: Differences in development and rates of JH biosynthesis between queen and worker larvae. J Insect Physiol. 1997;43: 373–381. doi:10.1016/S0022-1910(96)00106-0

81. Cnaani J, Robinson GE, Hefetz A. The critical period for caste determination in Bombus terrestris and its juvenile hormone correlates. J Comp Physiol - A Sensory, Neural, Behav Physiol. 2000;186: 1089–1094. doi:10.1007/s003590000163

82. Rajakumar R, San Mauro D, Dijkstra MB, Huang MH, Wheeler DE, Hiou-Tim F, et al. Ancestral Developmental Potential Facilitates Parallel Evolution in Ants. Science. 2012;335: 79–82. doi:10.1126/science.1211451

83. Linksvayer TA, Kaftanoglu O, Akyol E, Blatch S, Amdam G V., Page RE. Larval and nurse worker control of developmental plasticity and the evolution of honey bee queen-worker dimorphism. J Evol Biol. 2011;24: 1939–1948. doi:10.1111/j.1420-9101.2011.02331.x

84. Villalta I, Blight O, Angulo E, Cerdá X, Boulay R. Early developmental processes limit socially mediated phenotypic plasticity in an ant. Behav Ecol Sociobiol. 2016;70: 285–291. doi:10.1007/s00265-015-2052-4

85. Mutti NS, Dolezal AG, Wolschin F, Mutti JS, Gill KS, Amdam G V. IRS and TOR nutrient-signaling pathways act via juvenile hormone to influence honey bee caste fate. J Exp Biol. 2011;214: 3977–3984. doi:10.1242/jeb.061499

86. Buttstedt A, Ihling CH, Pietzsch M, Moritz RFA. Royalactin is not a royal making of a queen. Nature. Nature Publishing Group; 2016; E10–E12. doi:10.1038/nature19349

87. Kucharski R, Foret S, Maleszka R. EGFR gene methylation is not involved in Royalactin controlled phenotypic polymorphism in honey bees. Sci Rep. 2015;5: 14070. doi:10.1038/srep14070

88. Kamakura M. Kamakura replies. Nature. 2016;537: E13–E13. doi:10.1038/nature19350
89. Zhang L, Boeren S, Hageman JA, Van Hooijdonk T, Vervoort J, Hettinga K. Bovine milk proteome in the first 9 days: Protein interactions in maturation of the immune and digestive system of the newborn. PLoS One. 2015;10: 1–19. doi:10.1371/journal.pone.0116710
90. Soroker V, Hefetz A. Hydrocarbon site of synthesis and circulation in the desert ant *Cataglyphis niger*. J Insect Physiol. 2000;46: 1097–1102. doi:10.1016/S0022-1910(99)00219-X
91. Goodman WG, Granger NA. Insect Development: Morphogenesis, Molting and Metamorphosis. In: Gilbert LI, editor. Elsevier Science; 2009. p. 305.
92. Parra-Peralbo E, Culi J. Drosophila lipophorin receptors mediate the uptake of neutral lipids in oocytes and imaginal disc cells by an endocytosis-independent mechanism. PLoS Genet. 2011;7. doi:10.1371/journal.pgen.1001297
93. Rodríguez-Vázquez M, Vaquero D, Parra-Peralbo E, Mejía-Morales JE, Culi J. Drosophila Lipophorin Receptors Recruit the Lipoprotein LTP to the Plasma Membrane to Mediate Lipid Uptake. PLoS Genet. 2015;11: e1005356. doi:10.1371/journal.pgen.1005356
94. Engelmann F, Mala J. The interactions between juvenile hormone (JH), lipophorin, vitellogenin, and JH esterases in two cockroach species. Insect Biochemistry and Molecular Biology. 2000. pp. 793–803. doi:10.1016/S0965-1748(00)00051-5
95. Suzuki R, Fujimoto Z, Shiotsuki T, Tsuchiya W, Momma M, Tase A, et al. Structural mechanism of JH delivery in hemolymph by JHBP of silkworm, *Bombyx mori*. Sci Rep. 2011;1: 133. doi:10.1038/srep00133
96. Amsalem E, Malka O, Grozinger C, Hefetz A. Exploring the role of juvenile hormone and vitellogenin in reproduction and social behavior in bumble bees. BMC Evol Biol. BMC Evolutionary Biology; 2014;14: 45. doi:10.1186/1471-2148-14-45
97. Turchinovich A, Tonevitsky AG, Burwinkel B. Extracellular miRNA: A Collision of Two Paradigms. Trends Biochem Sci. Elsevier Ltd; 2016;41: 883–892. doi:10.1016/j.tibs.2016.08.004
98. Masood M, Everett CP, Chan SY, Snow JW. Negligible uptake and transfer of diet-derived pollen microRNAs in adult honey bees. RNA Biol. 2016;13: 109–118. doi:10.1080/15476286.2015.1128063
99. Rayner KJ, Hennessy EJ. Extracellular communication via microRNA: lipid particles have a new message. J Lipid Res May. 2013;54: 1174–1181. doi:10.1194/jlr.R034991

100. Alon U. An Introduction to Systems Biology: Design Principles of Biological Circuits. Chapman HallCRC mathematical and computational biology series. 2007. doi:citeulike-article-id:1314150

101. Hammock B, Nowock J, Gooddman W, Stamoudis V, Gilbert LI. The influence of hemolymph-binding protein on juvenile hormone stability and distribution in Manduca sexta fat body and imaginal discs in vitro. Mol Cell Endocrinol. 1975;3: 167–184. doi:10.1016/0303-7207(75)90043-X

102. Ward VK, Bonning BC, Huang T, Shiotsuki T, Griffeth VN, Hammock BD. Analysis of the catalytic mechanism of juvenile hormone esterase by site-directed mutagenesis. Int J Biochem. 1992;24: 1933–1941. Available: http://www.ncbi.nlm.nih.gov/pubmed/1473606

103. Campbell PM, Oakeshott JG, Healy MJ. Purification and kinetic characterisation of juvenile hormone esterase from Drosophila melanogaster. Insect Biochem Mol Biol. 1998;28: 501–515. doi:10.1016/S0965-1748(98)00037-X

104. Chertemps T, François A, Durand N, Rosell G, Dekker T, Lucas P, et al. A carboxylesterase, Esterase-6, modulates sensory physiological and behavioral response dynamics to pheromone in Drosophila. BMC Biol. 2012;10: 56. doi:10.1186/1741-7007-10-56

105. Costa R. Esterase-6 and the pheromonal effects of cis-vaccenyl acetate in *Drosophila melanogaster*. J Evol Biol. 1989;2: 395–407. doi:10.1046/j.1420-9101.1989.2060395.x

106. Flatt T, Tu M-P, Tatar M. Hormonal pleiotropy and the juvenile hormone regulation of Drosophila development and life history. BioEssays. 2005;27: 999–1010. doi:10.1002/bies.20290

107. Jindra M, Palli SR, Riddiford LM. The Juvenile Hormone Signaling Pathway in Insect Development. Annu Rev Entomol. 2013;58: 181–204. doi:10.1146/annurev-ento-120811-153700

108. Dolezal AG, Brent CS, Holldobler B, Amdam G V. Worker division of labor and endocrine physiology are associated in the harvester ant, *Pogonomyrmex californicus*. Journal of Experimental Biology. 2012. pp. 454–460. doi:10.1242/jeb.060822

109. Wang Y, Brent CS, Fennern E, Amdam G V. Gustatory perception and fat body energy metabolism are jointly affected by vitellogenin and juvenile hormone in honey bees. PLoS Genet. 2012;8. doi:10.1371/journal.pgen.1002779

110. Mersch DP, Crespi A, Keller L. Tracking individuals shows spatial fidelity is a key regulator of ant social organization. Science. 2013;340: 1090–3. doi:10.1126/science.1234316

111. Zybailov B, Mosley AL, Sardiu ME, Coleman MK, Florens L, Washburn MP. Statistical analysis of membrane proteome expression changes in *Saccharomyces cerevisiae*. J Proteome Res. 2006;5: 2339–2347. doi:10.1021/pr060161n
112. Wang L, Han X, Mehren J, Hiroi M, Billeter J-C, Miyamoto T, et al. Hierarchical chemosensory regulation of male-male social interactions in Drosophila. Nat Neurosci. 2011;14: 757–62. doi:10.1038/nn.2800
113. Le Conte Y, Mohammedi A, Robinson GE. Primer effects of a brood pheromone on honeybee behavioural development. Proc Biol Sci. 2001;268: 163–8. doi:10.1098/rspb.2000.1345
114. Mohammedi A, Crauser D, Paris A, Le Conte Y. Effect of a brood pheromone on honeybee hypopharyngeal glands. Comptes rendus de l'Académie des sciences. Série III, Sciences de la vie. 1996. pp. 769–72.
115. Choe D-H, Millar JG, Rust MK. Chemical signals associated with life inhibit necrophoresis in Argentine ants. Proc Natl Acad Sci. 2009;106: 8251–8255. doi:10.1073/pnas.0901270106
116. Shevchenko A, Tomas H, Havlis J, Olsen J V, Mann M. In-gel digestion for mass spectrometric characterization of proteins and proteomes. Nat Protoc. 2006;1: 2856–2860. doi:10.1038/nprot.2006.468
117. Keller A, Nesvizhskii AI, Kolker E, Aebersold R. Empirical statistical model to estimate the accuracy of peptide identifications made by MS/MS and database search. Anal Chem. 2002;74: 5383–5392. doi:10.1021/ac025747h
118. Nesvizhskii AI, Keller A, Kolker E, Aebersold R. A statistical model for identifying proteins by tandem mass spectrometry. Anal Chem. 2003;75: 4646–4658. doi:10.1021/ac0341261
119. Petersen TN, Brunak S, von Heijne G, Nielsen H. SignalP 4.0: discriminating signal peptides from transmembrane regions. Nat Methods. 2011;8: 785–6. doi:10.1038/nmeth.1701
120. Sapetschnig A, Sarkies P, Lehrbach NJ, Miska EA. Tertiary siRNAs Mediate Paramutation in *C. elegans*. PLoS Genet. 2015;11. doi:10.1371/journal.pgen.1005078
121. Linstrom PJ, Mallard WG. NIST Chemistry WebBook, NIST Standard Reference Database Number 69. NIST Chemistry WebBook. 2000. doi:citeulike-article-id:3211271
122. Kamita SG, Samra AI, Liu JY, Cornel AJ, Hammock BD. Juvenile hormone (JH) esterase of the mosquito *Culex quinquefasciatus* is not a target of the JH analog insecticide methoprene. PLoS One. 2011;6. doi:10.1371/journal.pone.0028392

123. Wallis DI. Spinning movements in the larvae of the ant, *Formica fusca*. Insectes Soc. 1960;7: 187–199. doi:10.1007/BF02224080

124. Grabherr MG, Haas BJ, Yassour M, Levin JZ, Thompson DA, Amit I, et al. Full-length transcriptome assembly from RNA-Seq data without a reference genome. Nat Biotechnol. 2011;29: 644–52. doi:10.1038/nbt.1883

125. Bolger AM, Lohse M, Usadel B. Trimmomatic: A flexible trimmer for Illumina sequence data. Bioinformatics. 2014;30: 2114–2120. doi:10.1093/bioinformatics/btu170

126. Altenhoff AM, Škunca N, Glover N, Train CM, Sueki A, Pilizota I, et al. The OMA orthology database in 2015: Function predictions, better plant support, synteny view and other improvements. Nucleic Acids Res. 2015;43: D240–D249. doi:10.1093/nar/gku1158

127. Stamatakis A. RAxML-VI-HPC: Maximum likelihood-based phylogenetic analyses with thousands of taxa and mixed models. Bioinformatics. 2006;22: 2688–2690. doi:10.1093/bioinformatics/btl446

Supplementary Figures and Tables

Figure 1- figure supplement 1. Proteomic characterization of *C. floridanus* trophallactic fluid. Heat map showing the percentage of total molecular weight-normalized spectra assigned to proteins from hemolymph, voluntary TF, forced TF or midgut fluids (normalized spectral abundance factor, NSAF [111]). C1-C10 indicate colony of origin. Forced trophallaxis samples are pooled from 10-20 ants, hemolymph from 30 ants, and the contents of dissected midguts from 5 ants each. Voluntary and midgut samples were collected from ants of multiple colonies. Approximately unbiased bootstrap probabilities for 10,000 repetitions are indicated by black circles where greater or equal to 95%. UniProt IDs are listed to the left and protein names to the right.

Figure 1-figure supplement 2. Social isolation influences trophallactic fluid content. Trophallaxis samples from the same ants, in-colony and group-isolated. Trophallactic fluid of ant workers sampled when first removed from the colony, then after 14 days of group isolation (~20-30 individuals per group). Values were normalized using spectral counting and the dendrogram shows approximately unbiased probabilities for 10,000 repetitions. Along the right side, UniProt IDs are shown. Proteins that significantly decreased in abundance in isolation are shown in orange, and proteins that increased in abundance are shown in green (t-test $p < 0.05$). Asterisks indicate Bonferroni-corrected t-test significance. Names in bold italics indicate proteins that significantly decreased in abundance in voluntary samples (socially isolated, starved then fed) relative to forced TF samples (in-colony) from data shown in Fig. 1A and figure supplement 1. Approximately unbiased (AU) bootstrap probabilities for 10,000 repetitions are indicated by black circles where greater or equal to 95% and grey circles where greater or equal to 75%.

Figure 3-figure supplement 1

(A) Typical GC-MS chromatogram of a TF sample from *C. floridanus*, showing the main hydrocarbons C28-C37 eluting after 40 min. The insert shows the region with minor hydrocarbons and other components C15-C28.

(B-D) GC-MS Mass spectra of linear alkane (n-hexacosane at Rt 34.69 min, panel B) and a dimethylated alkane at Rt 43.29 min (C). Extracted MS profiles were fitted with an exponential decay equation (B, D). The proposed structure for the branched alkane based on fragments ions (141 and 309) is 9,20-dimethyl nonacosane (D).

(E) RI values vs. number of carbons extracted from the NIST Chemistry WebBook library, depending on the number of ramifications: linear (black), monomethyl (red), dimethyl (blue), trimethyl (pink), tetramethyl (green) and pentamethyl (dark blue).

(F) The black dots represent experimental retention times with the calculated RI index for all identified hydrocarbons of the TF sample. The red dots represent the experimental retention times and with their RI index for the linear C8-C40 alkane standard.

Figure 3-source data 1.

Peak lists for cuticular and trophallactic fluid long chain hydrocarbons form GC-MS experiments for five different colonies of *C. floridanus*. C11, 20 ants, 9.5 µl of TF; C12, 38 ants, 20 µl; C13, 34 ants, 11 µl; C14, 26 ants, 11.5 µl; C15, 35 ants, 9 µl.

Figure 3-source data 2. Cross-correlation matrix for panels 3D-E.

Figure 4-source data 1. Hemolymph and trophallactic fluid Juvenile Hormone titers for 20 pooled samples of each fluid.

Figure 4-source data 2. Juvenile Hormone titers for 37 individual third instar larvae.

Figure 4-source data 3. Head-width measurements for panel 4C.

Figure 4-source data 4. Metamorphosis or death counts for panel 4D.

Figure 5–figure supplement 1

Heat map showing the percentage of total molecular-weight normalized spectra in trophallactic fluid samples assigned to each protein in three ant species and the European honey bee,

averaged over all in-colony samples for that species. Sample sizes: *C. floridanus* (n=15), *C. fellah* (n=6), *S. invicta* (n=3), *A. mellifera* (n=6). The 26 protein ortholog groups whose presence/absence in TF was inconsistent with phylogeny (e.g., present in only *C. floridanus* and *A. mellifera*) are shown in orange. Protein names are shown on the left. Identifiers can be found in the table in Figure 5–figure supplement 2.

Figure 5-source data 1

A table of all orthologous proteins and their predicted functions, identifiers, known *D. melanogaster* orthologs, presence of annotated secretion signals and average NSAF values when present in TF. A complete orthology across the four species can be found in Supplementary File 3.

Supplemental File 1. RNA of microorganisms present in trophallactic fluid.

Supplemental File 2. Proteomic experiments included in this study.

Supplemental File 3. Orthology matrix across four social insect species.

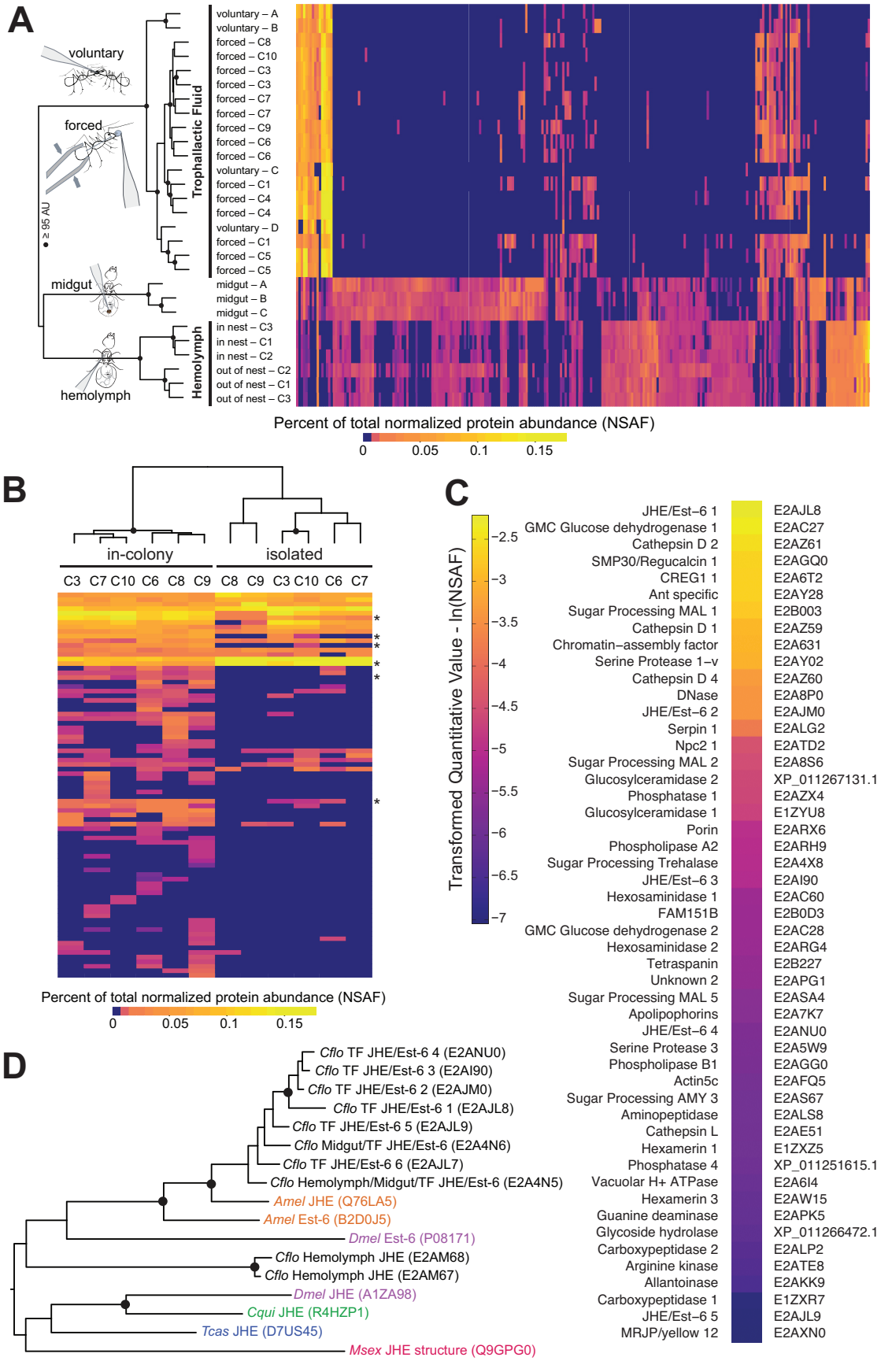
A
voluntary
forced
midgut
hemolymph
≥ 95 AU
Trophallactic Fluid
Hemolymph
voluntary – A
voluntary – B
forced – C8
forced – C10
forced – C3
forced – C3
forced – C7
forced – C7
forced – C9
forced – C6
forced – C6
voluntary – C
forced – C1
forced – C4
forced – C4
voluntary – D
forced – C1
forced – C5
forced – C5
midgut – A
midgut – B
midgut – C
in nest – C3
in nest – C1
in nest – C2
out of nest – C2
out of nest – C1
out of nest – C3
Percent of total normalized protein abundance (NSAF)
0
0.05
0.1
0.15
B
in-colony
isolated
C3 C7 C10 C6 C8 C9
C8 C9 C3 C10 C6 C7
Percent of total normalized protein abundance (NSAF)
0
0.05
0.1
0.15
C
Transformed Quantitative Value - ln(NSAF)
−2.5
−3
−3.5
−4
−4.5
−5
−5.5
−6
−6.5
−7
JHE/Est−6 1
GMC Glucose dehydrogenase 1
Cathepsin D 2
SMP30/Regucalcin 1
CREG1 1
Ant specific
Sugar Processing MAL 1
Cathepsin D 1
Chromatin−assembly factor
Serine Protease 1−v
Cathepsin D 4
DNase
JHE/Est−6 2
Serpin 1
Npc2 1
Sugar Processing MAL 2
Glucosylceramidase 2
Phosphatase 1
Glucosylceramidase 1
Porin
Phospholipase A2
Sugar Processing Trehalase
JHE/Est−6 3
Hexosaminidase 1
FAM151B
GMC Glucose dehydrogenase 2
Hexosaminidase 2
Tetraspanin
Unknown 2
Sugar Processing MAL 5
Apolipophorins
JHE/Est−6 4
Serine Protease 3
Phospholipase B1
Actin5c
Sugar Processing AMY 3
Aminopeptidase
Cathepsin L
Hexamerin 1
Phosphatase 4
Vacuolar H+ ATPase
Hexamerin 3
Guanine deaminase
Glycoside hydrolase
Carboxypeptidase 2
Arginine kinase
Allantoinase
Carboxypeptidase 1
JHE/Est−6 5
MRJP/yellow 12
E2AJL8
E2AC27
E2AZ61
E2AGQ0
E2A6T2
E2AY28
E2B003
E2AZ59
E2A631
E2AY02
E2AZ60
E2A8P0
E2AJM0
E2ALG2
E2ATD2
E2A8S6
XP_011267131.1
E2AZX4
E1ZYU8
E2ARX6
E2ARH9
E2A4X8
E2AI90
E2AC60
E2B0D3
E2AC28
E2ARG4
E2B227
E2APG1
E2ASA4
E2A7K7
E2ANU0
E2A5W9
E2AGG0
E2AFQ5
E2AS67
E2ALS8
E2AE51
E1ZXZ5
XP_011251615.1
E2A6I4
E2AW15
E2APK5
XP_011266472.1
E2ALP2
E2ATE8
E2AKK9
E1ZXR7
E2AJL9
E2AXN0
D
Cflo TF JHE/Est-6 4 (E2ANU0)
Cflo TF JHE/Est-6 3 (E2AI90)
Cflo TF JHE/Est-6 2 (E2AJM0)
Cflo TF JHE/Est-6 1 (E2AJL8)
Cflo TF JHE/Est-6 5 (E2AJL9)
Cflo Midgut/TF JHE/Est-6 (E2A4N6)
Cflo TF JHE/Est-6 6 (E2AJL7)
Cflo Hemolymph/Midgut/TF JHE/Est-6 (E2A4N5)
Amel JHE (Q76LA5)
Amel Est-6 (B2D0J5)
Dmel Est-6 (P08171)
Cflo Hemolymph JHE (E2AM68)
Cflo Hemolymph JHE (E2AM67)
Dmel JHE (A1ZA98)
Cqui JHE (R4HZP1)
Tcas JHE (D7US45)
Msex JHE structure (Q9GPG0)

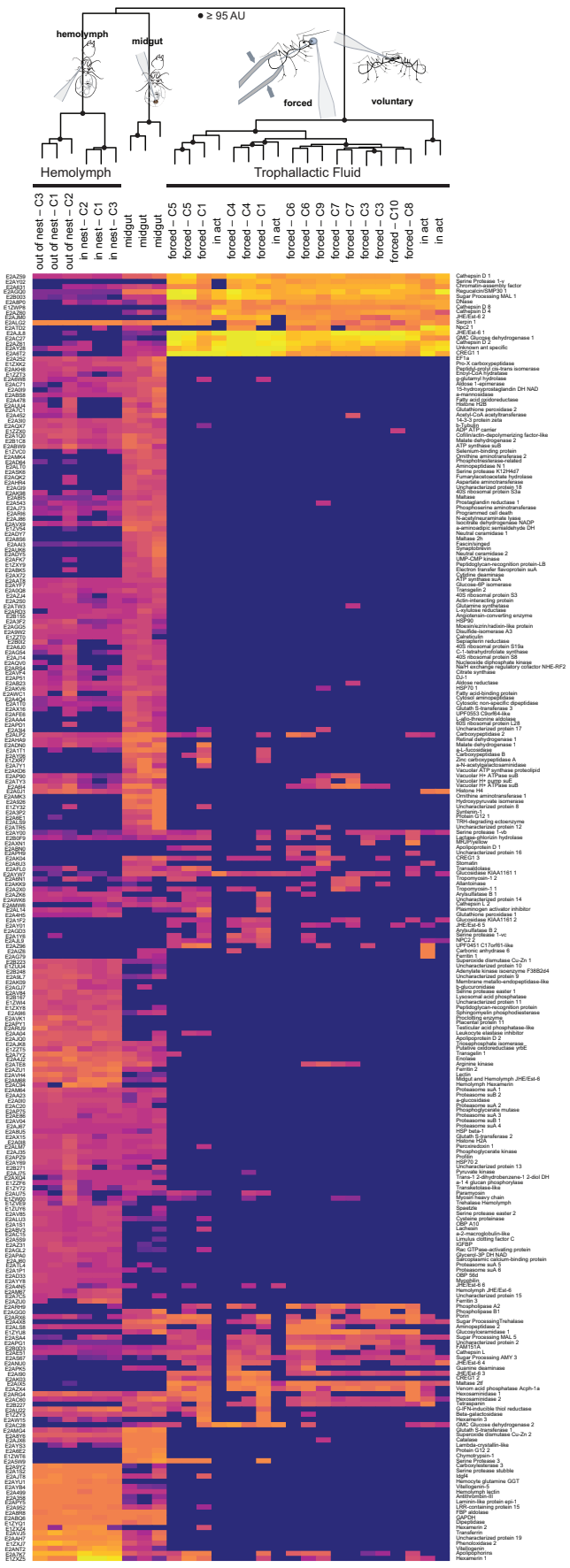
≥ 95 AU
hemolymph
midgut
forced
voluntary
Hemolymph
Trophallactic Fluid
out of nest – C3
out of nest – C1
out of nest – C2
in nest – C2
in nest – C1
in nest – C3
midgut
midgut
midgut
forced – C5
forced – C5
forced – C1
in act
forced – C4
forced – C4
forced – C1
in act
forced – C6
forced – C6
forced – C9
forced – C7
forced – C7
forced – C3
forced – C3
forced – C10
forced – C8
in act
in act

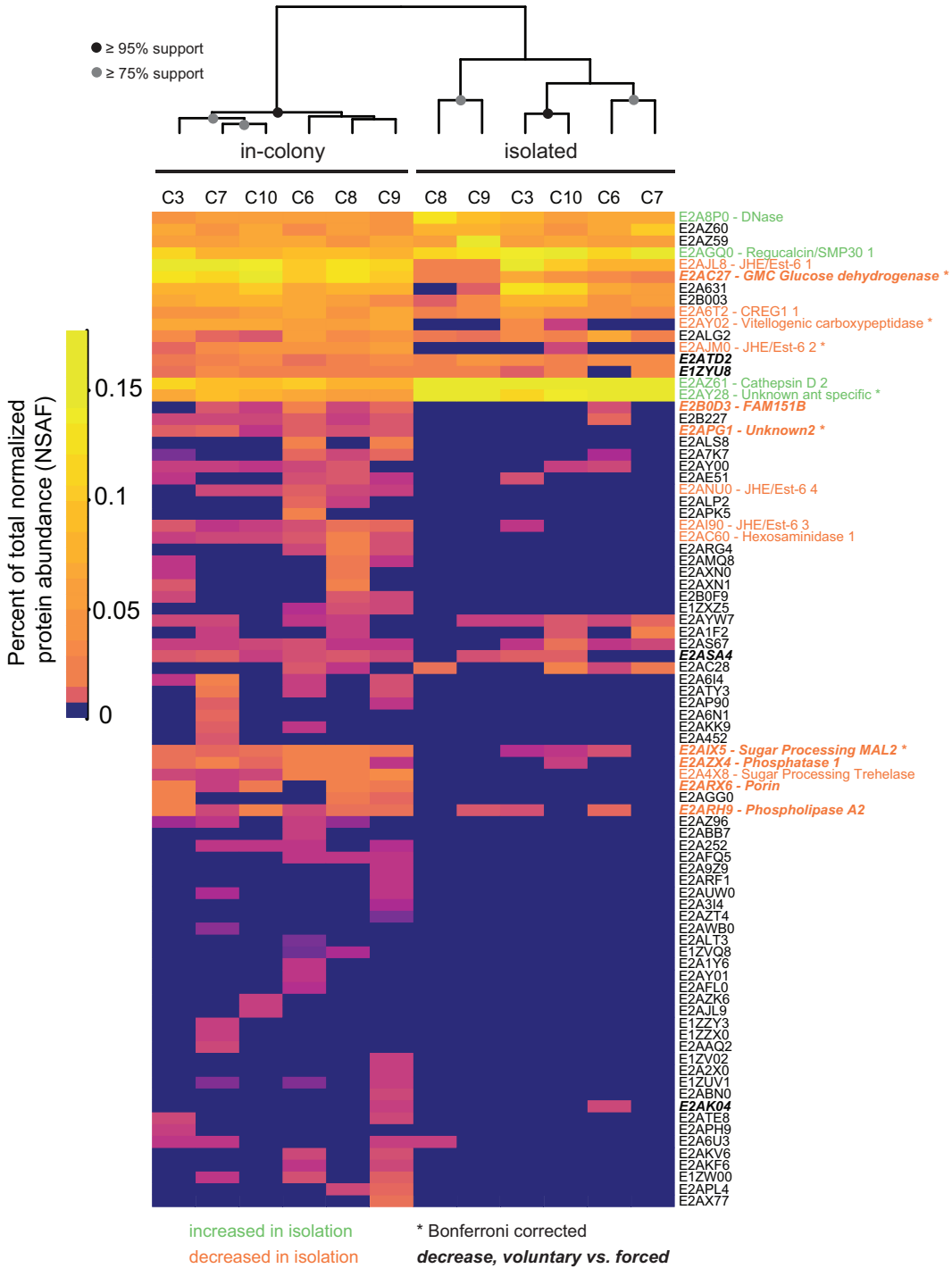
≥ 95% support
≥ 75% support
in-colony
isolated
C3 C7 C10 C6 C8 C9 C8 C9 C3 C10 C6 C7
Percent of total normalized protein abundance (NSAF)
0.15
0.1
0.05
0
E2A8P0 - DNase
E2AZ60
E2AZ59
E2AGQ0 - Regucalcin/SMP30 1
E2AJL8 - JHE/Est-6 1
E2AC27 - GMC Glucose dehydrogenase *
E2A631
E2B003
E2A6T2 - CREG1 1
E2AY02 - Vitellogenic carboxypeptidase *
E2ALG2
E2AJM0 - JHE/Est-6 2 *
E2ATD2
E1ZYU8
E2AZ61 - Cathepsin D 2
E2AY28 - Unknown ant specific *
E2B0D3 - FAM151B
E2B227
E2APG1 - Unknown2 *
E2ALS8
E2A7K7
E2AY00
E2AE51
E2ANU0 - JHE/Est-6 4
E2ALP2
E2APK5
E2AI90 - JHE/Est-6 3
E2AC60 - Hexosaminidase 1
E2ARG4
E2AMQ8
E2AXN0
E2AXN1
E2B0F9
E1ZXZ5
E2AYW7
E2A1F2
E2AS67
E2ASA4
E2AC28
E2A6I4
E2ATY3
E2AP90
E2A6N1
E2AKK9
E2A452
E2AIX5 - Sugar Processing MAL2 *
E2AZX4 - Phosphatase 1
E2A4X8 - Sugar Processing Trehelase
E2ARX6 - Porin
E2AGG0
E2ARH9 - Phospholipase A2
E2AZ96
E2ABB7
E2A252
E2AFQ5
E2A9Z9
E2ARF1
E2AUW0
E2A3I4
E2AZT4
E2AWB0
E2ALT3
E1ZVQ8
E2A1Y6
E2AY01
E2AFL0
E2AZK6
E2AJL9
E1ZZY3
E1ZZX0
E2AAQ2
E1ZV02
E2A2X0
E1ZUV1
E2ABN0
E2AK04
E2ATE8
E2APH9
E2A6U3
E2AKV6
E2AKF6
E1ZW00
E2APL4
E2AX77
increased in isolation
decreased in isolation
* Bonferroni corrected
decrease, voluntary vs. forced

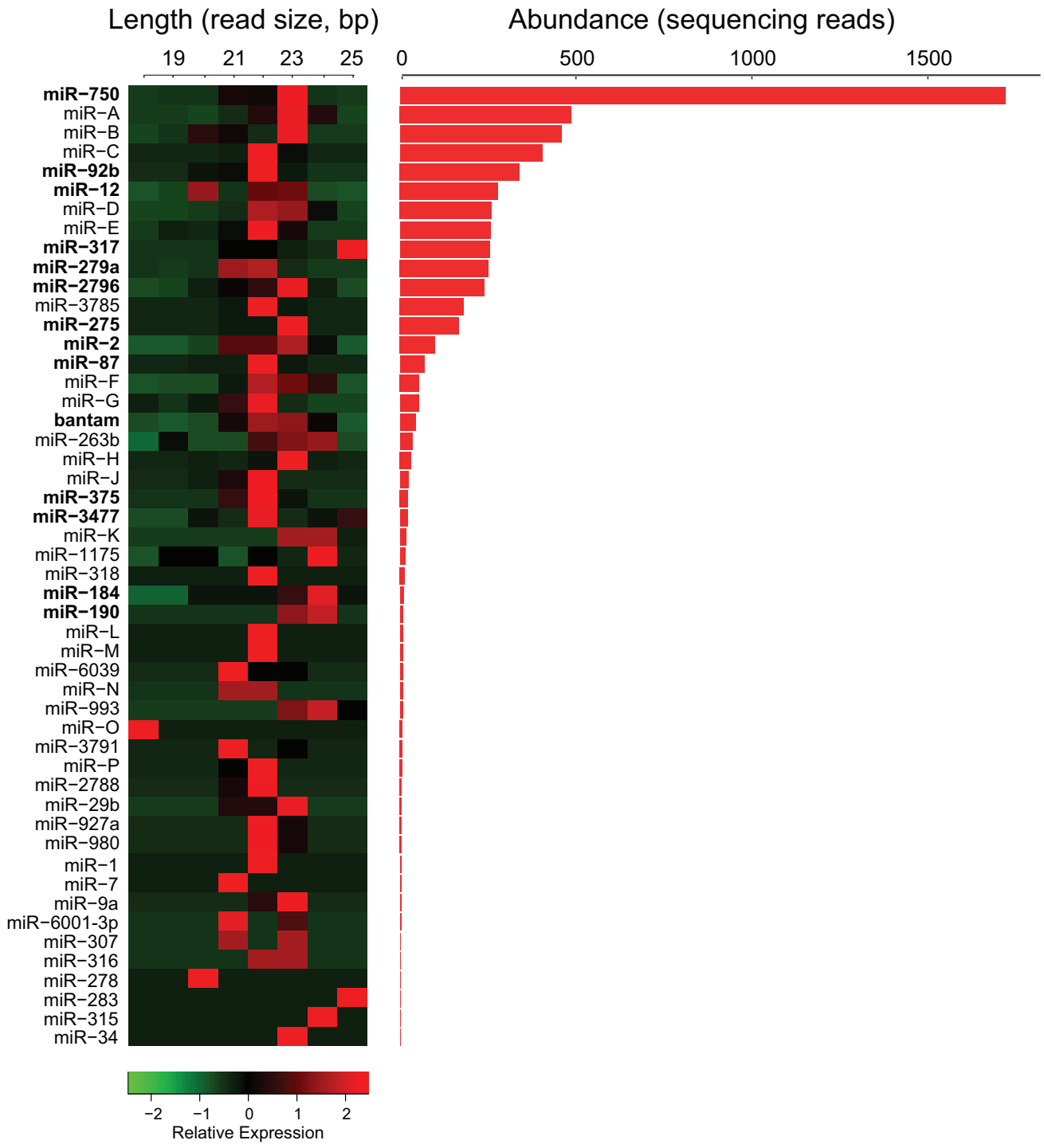
Length (read size, bp)
19
21
23
25
Abundance (sequencing reads)
0
500
1000
1500
miR−750
miR−A
miR−B
miR−C
miR−92b
miR−12
miR−D
miR−E
miR−317
miR−279a
miR−2796
miR−3785
miR−275
miR−2
miR−87
miR−F
miR−G
bantam
miR−263b
miR−H
miR−J
miR−375
miR−3477
miR−K
miR−1175
miR−318
miR−184
miR−190
miR−L
miR−M
miR−6039
miR−N
miR−993
miR−O
miR−3791
miR−P
miR−2788
miR−29b
miR−927a
miR−980
miR−1
miR−7
miR−9a
miR−6001-3p
miR−307
miR−316
miR−278
miR−283
miR−315
miR−34
−2
−1
0
1
2
Relative Expression

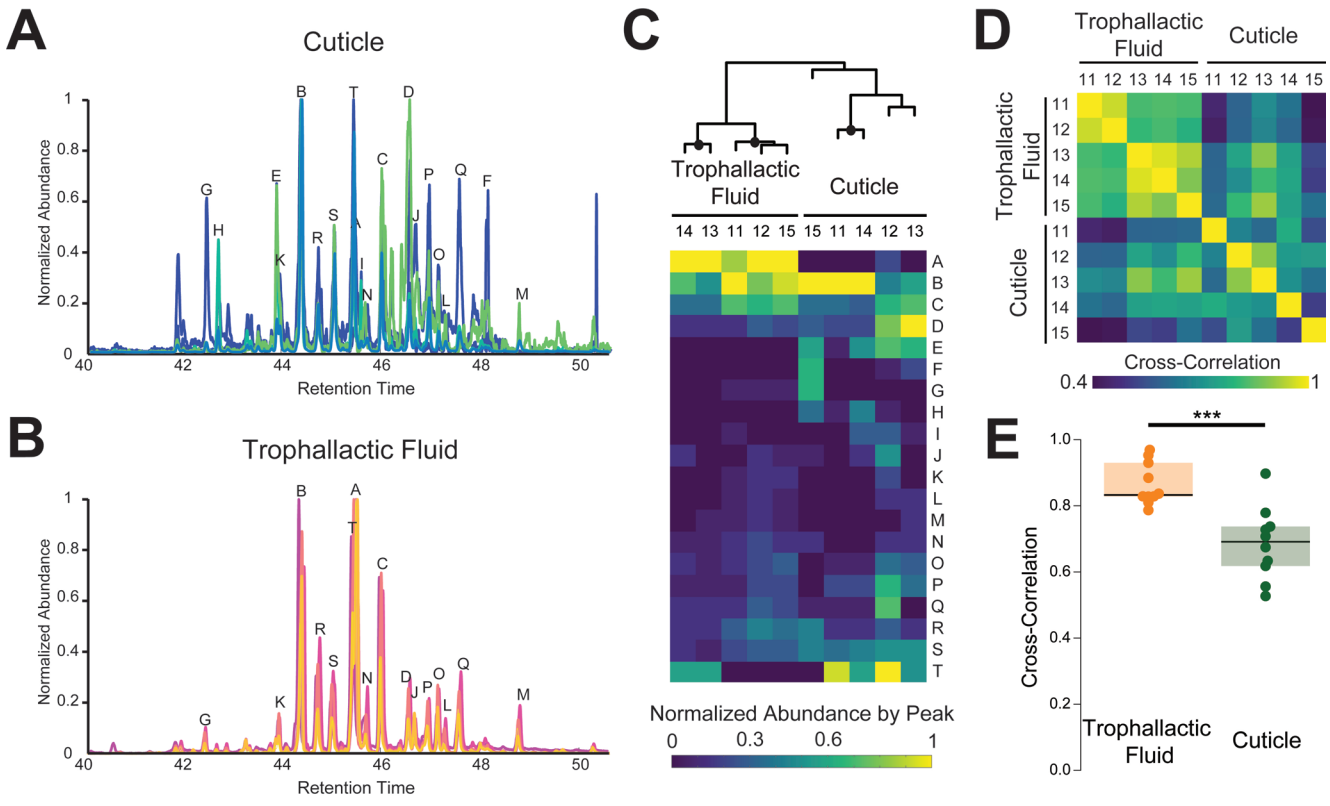
A
Cuticle
Normalized Abundance
Retention Time
B
Trophallactic Fluid
Normalized Abundance
Retention Time
C
Trophallactic Fluid
Cuticle
Normalized Abundance by Peak
0
0.3
0.6
1
D
Trophallactic Fluid
Cuticle
Cross-Correlation
0.4
1
E
***
Cross-Correlation
Trophallactic Fluid
Cuticle

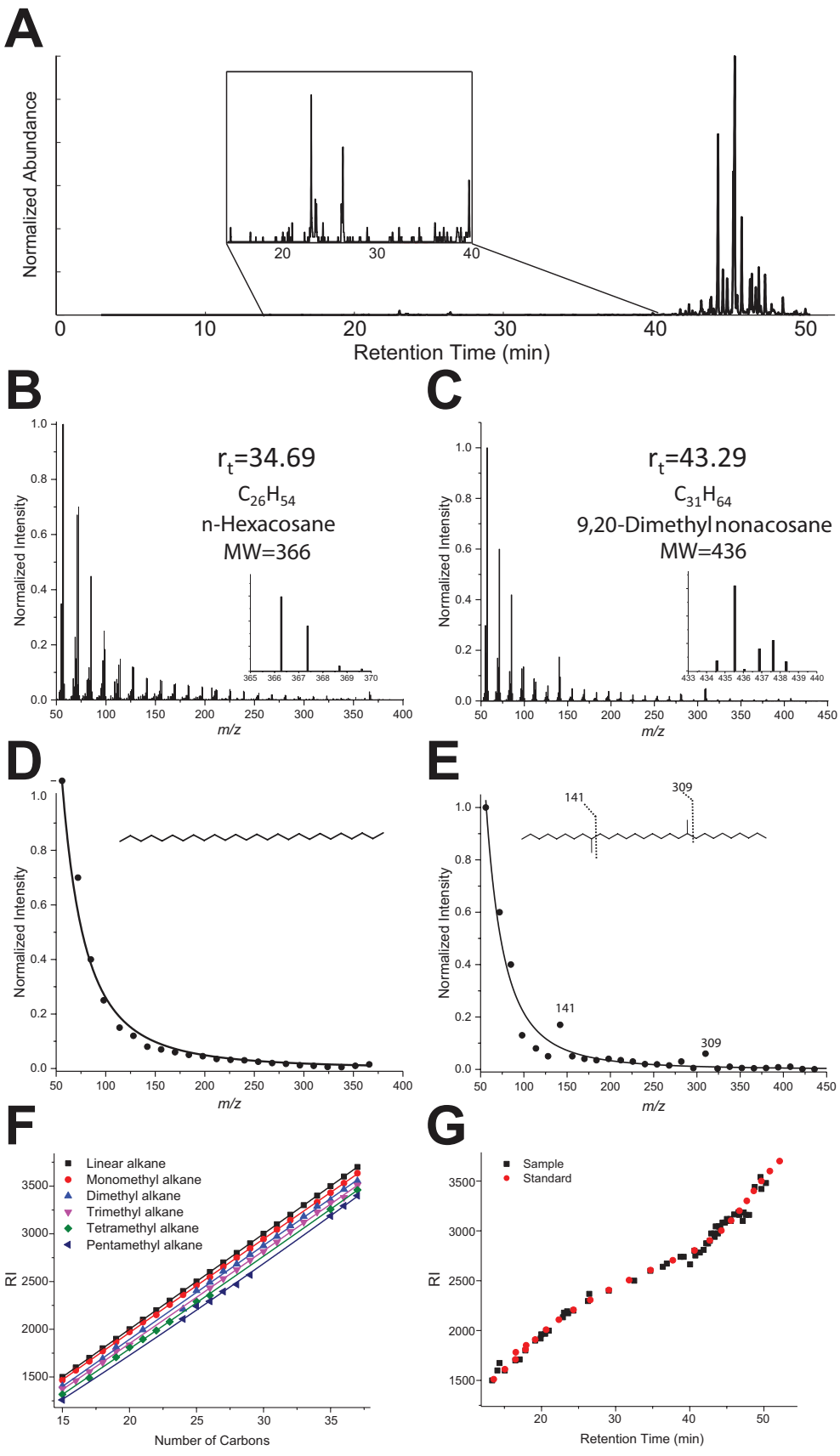
A
Normalized Abundance
Retention Time (min)
B
r_t=34.69
$C_{26}H_{54}$
n-Hexacosane
MW=366
Normalized Intensity
m/z
C
r_t=43.29
$C_{31}H_{64}$
9,20-Dimethylnonacosane
MW=436
Normalized Intensity
m/z
D
Normalized Intensity
m/z
E
141
309
Normalized Intensity
m/z
F
Linear alkane
Monomethyl alkane
Dimethyl alkane
Trimethyl alkane
Tetramethyl alkane
Pentamethyl alkane
RI
Number of Carbons
G
Sample
Standard
RI
Retention Time (min)

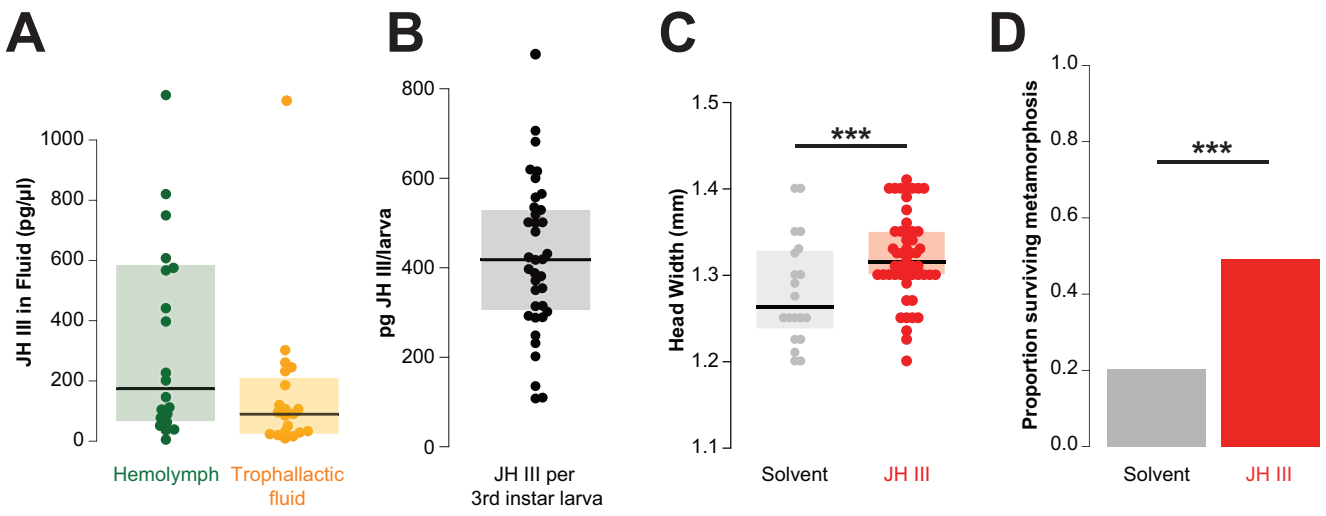
A
JH III in Fluid (pg/µl)
1000
800
600
400
200
0
Hemolymph
Trophallactic fluid
B
pg JH III/larva
800
600
400
200
0
JH III per 3rd instar larva
C
Head Width (mm)
1.5
1.4
1.3
1.2
1.1
***
Solvent
JH III
D
Proportion surviving metamorphosis
1.0
0.8
0.6
0.4
0.2
0.0
***
Solvent
JH III

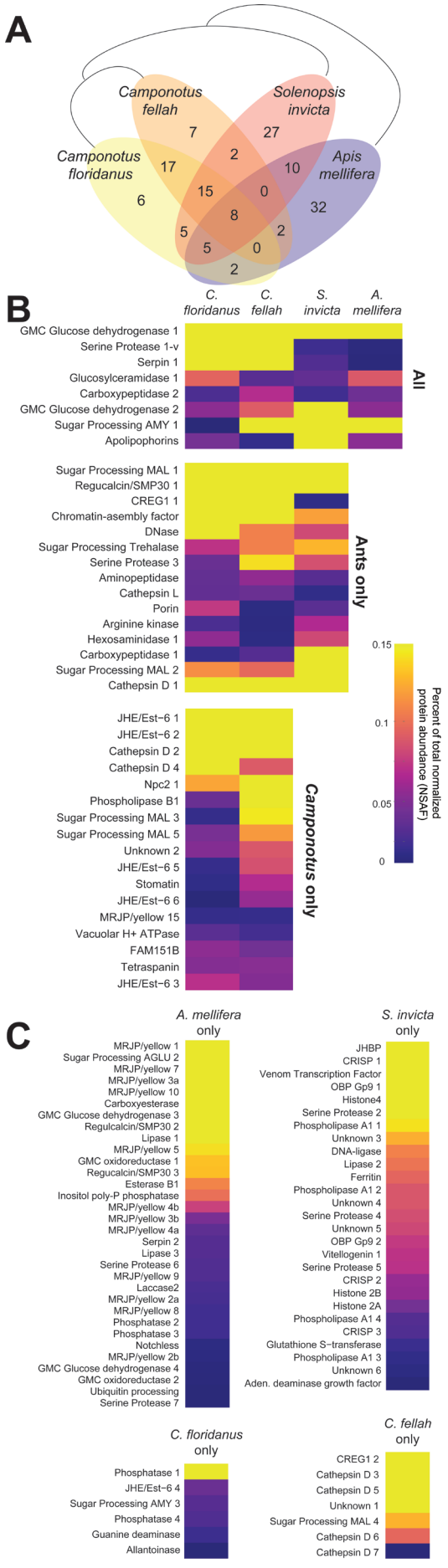
A
Camponotus fellah
Solenopsis invicta
Camponotus floridanus
Apis mellifera
7
27
2
17
10
15
0
6
8
32
5
2
5
0
2
B
C. floridanus
C. fellah
S. invicta
A. mellifera
GMC Glucose dehydrogenase 1
Serine Protease 1-v
Serpin 1
Glucosylceramidase 1
Carboxypeptidase 2
GMC Glucose dehydrogenase 2
Sugar Processing AMY 1
Apolipophorins
All
Sugar Processing MAL 1
Regucalcin/SMP30 1
CREG1 1
Chromatin-asembly factor
DNase
Sugar Processing Trehalase
Serine Protease 3
Aminopeptidase
Cathepsin L
Porin
Arginine kinase
Hexosaminidase 1
Carboxypeptidase 1
Sugar Processing MAL 2
Cathepsin D 1
Ants only
JHE/Est−6 1
JHE/Est−6 2
Cathepsin D 2
Cathepsin D 4
Npc2 1
Phospholipase B1
Sugar Processing MAL 3
Sugar Processing MAL 5
Unknown 2
JHE/Est−6 5
Stomatin
JHE/Est−6 6
MRJP/yellow 15
Vacuolar H+ ATPase
FAM151B
Tetraspanin
JHE/Est−6 3
Camponotus only
0.15
0.1
0.05
0
Percent of total normalized protein abundance (NSAF)
C
A. mellifera only
MRJP/yellow 1
Sugar Processing AGLU 2
MRJP/yellow 7
MRJP/yellow 3a
MRJP/yellow 10
Carboxyesterase
GMC Glucose dehydrogenase 3
Regulcalcin/SMP30 2
Lipase 1
MRJP/yellow 5
GMC oxidoreductase 1
Regucalcin/SMP30 3
Esterase B1
Inositol poly-P phosphatase
MRJP/yellow 4b
MRJP/yellow 3b
MRJP/yellow 4a
Serpin 2
Lipase 3
Serine Protease 6
MRJP/yellow 9
Laccase2
MRJP/yellow 2a
MRJP/yellow 8
Phosphatase 2
Phosphatase 3
Notchless
MRJP/yellow 2b
GMC Glucose dehydrogenase 4
GMC oxidoreductase 2
Ubiquitin processing
Serine Protease 7
S. invicta only
JHBP
CRISP 1
Venom Transcription Factor
OBP Gp9 1
Histone4
Serine Protease 2
Phospholipase A1 1
Unknown 3
DNA-ligase
Lipase 2
Ferritin
Phospholipase A1 2
Unknown 4
Serine Protease 4
Unknown 5
OBP Gp9 2
Vitellogenin 1
Serine Protease 5
CRISP 2
Histone 2B
Histone 2A
Phospholipase A1 4
CRISP 3
Glutathione S−transferase
Phospholipase A1 3
Unknown 6
Aden. deaminase growth factor
C. floridanus only
Phosphatase 1
JHE/Est−6 4
Sugar Processing AMY 3
Phosphatase 4
Guanine deaminase
Allantoinase
C. fellah only
CREG1 2
Cathepsin D 3
Cathepsin D 5
Unknown 1
Sugar Processing MAL 4
Cathepsin D 6
Cathepsin D 7


C. floridanus
C. fellah
S. invicta
A. mellifera
Cathepsin D 1
Ant specific
Chromatin-assembly factor
Serine Protease 1-v
DNase
Cathepsin D 4
Cathepsin D 2
CREG1 1
JHE/Est-6 1
GMC Glucose dehydrogenase 1
SMP30/Regucalcin 1
Sugar Processing MAL 1
JHE/Est-6 2
Sugar Processing AGLU 1
Sugar Processing AGLU 2
MRJP/yellow 7
MRJP/yellow 3a
MRJP/yellow 10
MRJP/yellow 1
Sugar Processing MAL 3
Sugar Processing MAL 4
Cathepsin D 6
Phospholipase B1
Sugar Processing MAL 5
Unknown 2
Serine Protease 3
Sugar Processing AMY 2
Sugar Processing Trehalase
Glucosylceramidase 3
Cathepsin D 7
JHE/Est-6 6
Stomatin
Npc2 2
JHE/Est-6 5
Carboxypeptidase 2
Serpin 1
Npc2 1
Tetraspanin
FAM151B
JHE/Est-6 3
Cathepsin L
Aminopeptidase
Sugar Processing AMY 3
Phosphatase 4
JHE/Est-6 4
Actin5c
Hexosaminidase 2
Guanine deaminase
Allantoinase
MRJP/yellow 12
Glycoside hydrolase
Glucosylceramidase 1
Glucosylceramidase 2
Porin
Phospholipase A2
Phosphatase 1
Serpin 2
Lipase 3
Serine Protease 6
MRJP/yellow 9
MRJP/yellow 4a
MRJP/yellow 3b
MRJP/yellow 8
Phosphatase 2
Phosphatase 3
Laccase2
MRJP/yellow 2a
Aldehyde oxidase
GMC Glucose dehydrogenase 4
GMC oxidoreductase 2
Ubiquitin processing
Serine Protease 7
Notchless
MRJP/yellow 2b
GMC oxidoreductase 1
SMP30/Regucalcin 3
MRJP/yellow 5
SMP30/Regucalcin 2
Lipase 1
Esterase B1
Inositol polyphosphate phosphatase 4
MRJP/yellow 4b
Carboxyesterase
GMC Glucose dehydrogenase 3
MRJP/yellow 6
CREG1 2
Cathepsin D 3
Cathepsin D 5
Unknown 1
Sugar Processing AMY 1
Apolipophorins
JHBP
Sugar Processing MAL 2
Venom Transcription Factor
OBP Gp9 1
Carboxypeptidase 1
Hexamerin 1
GMC Glucose dehydrogenase 2
CRISP 1
Phospholipase A1 2
Unknown 4
Hexamerin 2
Ferritin
Chitinase
Serine Protease 4
Unknown 5
Vhdl, vitellogenin-like
Lipase 2
DNA-ligase
Vitellogenin 1
Serine Protease 5
OBP Gp9 2
Prophenoloxidase
CRISP 2
Histone 2B
Lectin
MRJP/yellow 11
Hexosaminidase 1
Serine Protease 2
Phospholipase A1 1
Unknown 3
Imaginal disc growth factor 4
Transferrin
Histone4
Phospholipase A1 4
CRISP 3
Metal protease
Glutathione peroxidase
Histone 2A
Arginine kinase
Phospholipase A1 3
Unknown 6
Glutathione S-transferase
GAPDH
Hexamerin 3
Icarapin